Additional Material for Solids-State Physics 1

Nicola Manini

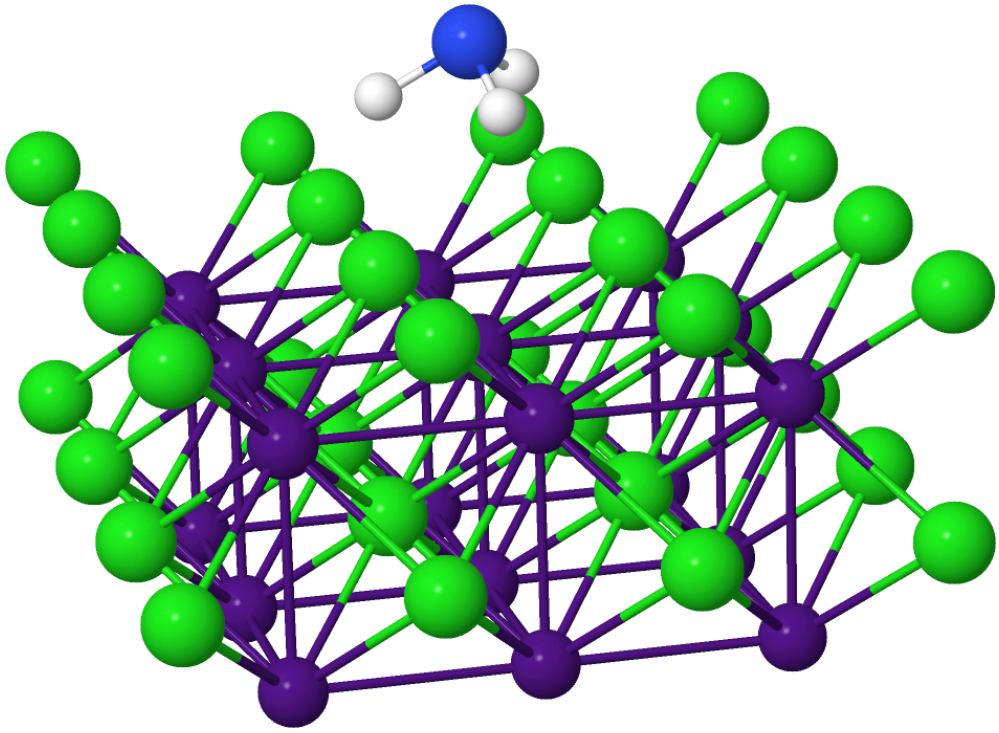

Version 0.96 – Mar 15, 2026

Introduction

The *Solid-state physics 1* course provides a general understanding of a broad range of fundamental phenomena and properties of solid-state matter.

The course covers the fundamental structural, electronic, vibrational, and spectroscopic properties of crystals, plus heat and electricity transport.

The main textbook is Kittel's *Introduction to Solid State Physics* [**1**].

We cherry-pick specific topics from Refs. [**2, 3, 4**].

The present Additional Material collects a few topics&figures either not covered in the suggest textbooks or simply handy to have and look at.

CHAPTER 1

Periodic structures and diffraction experiments

1.1. Bravais lattices and crystalline structures

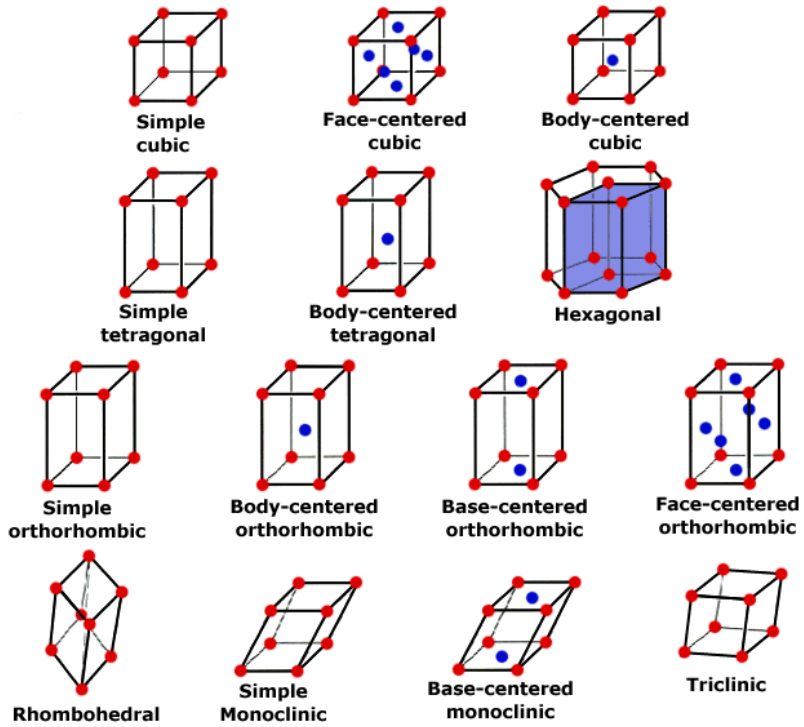

FIGURE 1.1. A sketch of the 14 Bravais lattices. According to their symmetry point group, they can be organized into 7 lattice systems, namely: cubic (3), tetragonal (2), hexagonal (1), orthorhombic (4), rhombohedral (1), monoclinic (2), and triclinic (1).

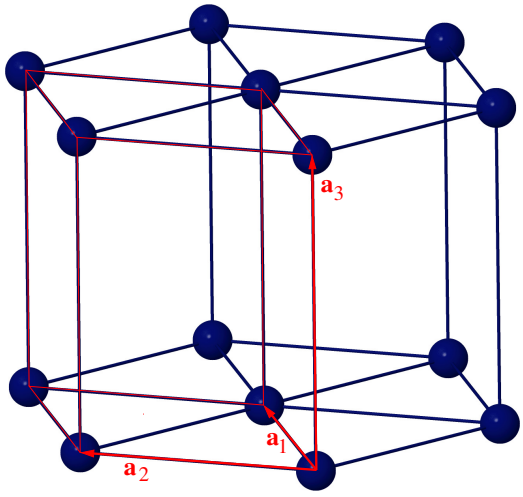

FIGURE 1.2. The hexagonal lattice: a possible choice of primitive vectors $\mathbf{a}_1 = a\hat{\mathbf{x}}$, $\mathbf{a}_2 = \frac{a}{2}(\hat{\mathbf{x}} + \sqrt{3}\hat{\mathbf{y}})$, $\mathbf{a}_3 = c\,\hat{\mathbf{z}}$; the parallelepiped cell $\sum_{i=1,2,3} x_i \mathbf{a}_i$ with $0 \le x_i < 1$ is a rhombic right prism with a 60° (or 120°) angle between $\mathbf{a}_1$ and $\mathbf{a}_2$. The cell volume $V_c = \frac{\sqrt{3}}{2} a^2 c$.

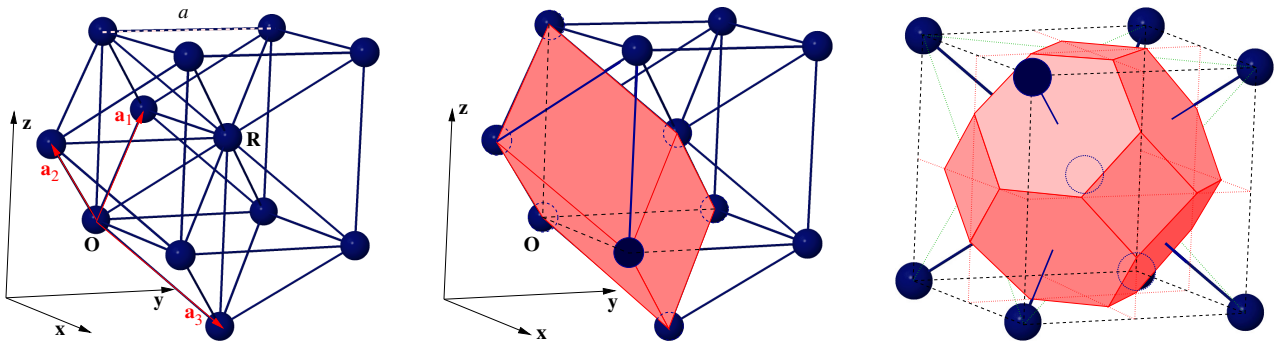

FIGURE 1.3. The bcc lattice: the standard primitive vectors $\mathbf{a}_1 = \frac{a}{2}(\hat{\mathbf{y}} + \hat{\mathbf{z}} - \hat{\mathbf{x}})$, $\mathbf{a}_2 = \frac{a}{2}(\hat{\mathbf{z}} + \hat{\mathbf{x}} - \hat{\mathbf{y}})$, $\mathbf{a}_3 = \frac{a}{2}(\hat{\mathbf{x}} + \hat{\mathbf{y}} - \hat{\mathbf{z}})$; the parallelepiped cell $\sum_{i=1,2,3} x_i \mathbf{a}_i$ with $0 \le x_i < 1$ is a rhombohedron with edge $\frac{\sqrt{3}}{2}a$ and angles between adjecent edges $= \arccos(-\frac{1}{3}) \simeq 109.471°$; and the Wigner-Seitz cell (a truncated octahedron). The cell volume $V_c = \frac{1}{2}a^3$.

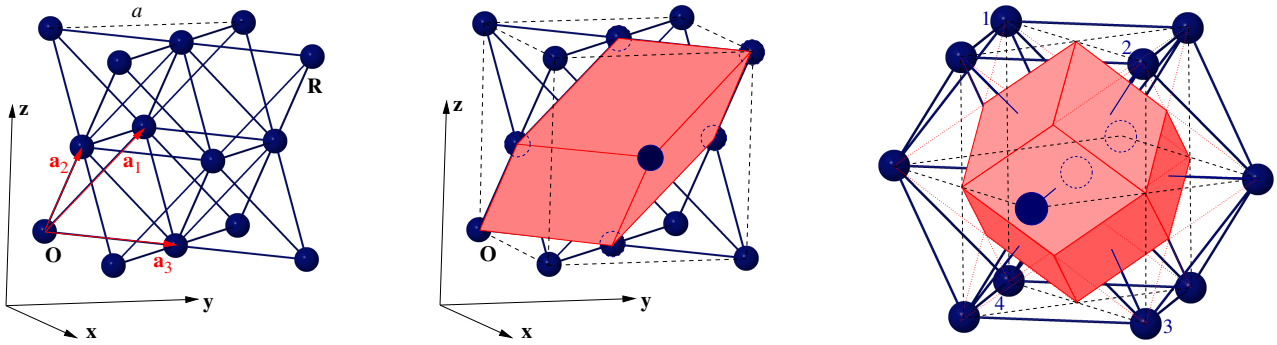

FIGURE 1.4. The fcc lattice: the standard primitive vectors $\mathbf{a}_1 = \frac{a}{2}(\hat{\mathbf{y}} + \hat{\mathbf{z}})$, $\mathbf{a}_2 = \frac{a}{2}(\hat{\mathbf{z}} + \hat{\mathbf{x}})$, $\mathbf{a}_3 = \frac{a}{2}(\hat{\mathbf{x}} + \hat{\mathbf{y}})$; the parallelepiped cell $\sum_{i=1,2,3} x_i \mathbf{a}_i$ with $0 \le x_i < 1$ is a rhombohedron with edge $\frac{a}{\sqrt{2}}$ and angles between adjecent edges $= 60°$; and the Wigner-Seitz cell (a rhombic dodecahedron). The cell volume $V_c = \frac{1}{4}a^3$.

1.2. Examples of crystalline structures

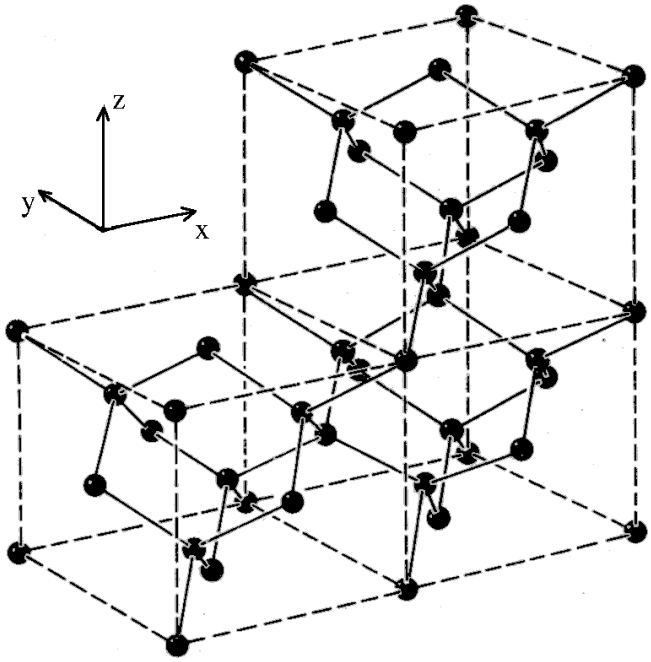

FIGURE 1.5. The diamond structure consists of two interpenetrating fcc Bravais lattices, displaced along the body diagonal of the cubic cell by one quarter of the length of this diagonal. In other words it is a fcc lattice with the two-atom basis $\mathbf{0}$ and $\frac{1}{4}(\mathbf{a}_1 + \mathbf{a}_2 + \mathbf{a}_3) = \frac{a}{4}(\hat{\mathbf{x}} + \hat{\mathbf{y}} + \hat{\mathbf{z}})$. 8 atoms reside in each conventional cubic cell. Four elements (C, Si, Ge, Sn) crystallize in this structure with lattice constants a = 3.56, 5.43, 5.65, and 6.46 Å, respectively.

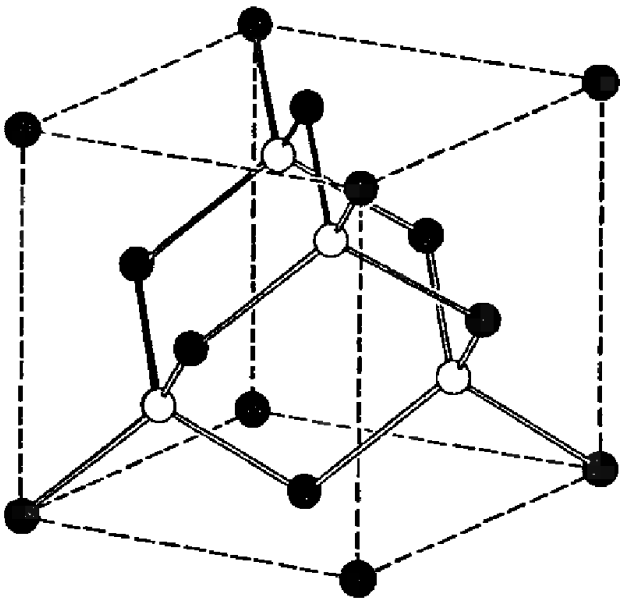

FIGURE 1.6. The zincblend structure is geometrically identical to the diamond structure with two chemically different atoms at the two inequivalent basis points in the fcc lattice cell. Common compounds that crystallize in the zincblend structure are listed below.

Crystal	a	Crystal	a
CuF	4.26 Å	ZnSe	5.65 Å
SiC	4.35	GaAs	5.65
CuCl	5.41	AlAs	5.66
ZnS	5.41	CdS	5.82
AlP	5.45	InSb	6.46
GaP	5.45	AgI	6.47

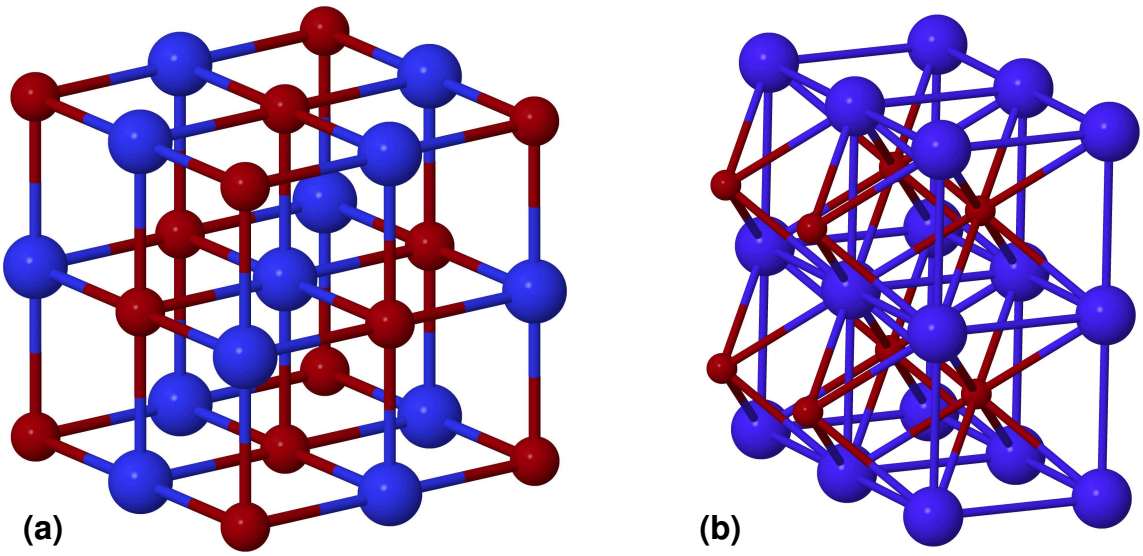

FIGURE 1.7. (a) The sodium chloride structure. (b) The cesium chloride structure. Small and large balls represent ions of two different types. In the NaCl crystal, the ions of each kind form interpenetrating fcc lattices: each ion is surrounded by 6 ions of the other kind. In the CsCl crystal, the ions of each kind form interpenetrating simple-cubic lattices: each ion is surrounded by 8 ions of the other kind.

1.3. Diffraction: elastic scattering from a crystal

Coherent elastic scattering of "radiation" (X rays or neutrons) from a piece of matter.

Summing coherently the scattered amplitudes at the detector, the total probability for the probing radiation to scatter from $\vec{k}$ to $\vec{k}'$ is proportional to the square modulus of

$$(1) \qquad \int e^{-i\vec{k}'\cdot\vec{r}}\, n(\vec{r})\, e^{i\vec{k}\cdot\vec{r}}\, d^3\vec{r} = \int e^{-i(\vec{k}'-\vec{k})\cdot\vec{r}}\, n(\vec{r})\, d^3\vec{r} = \int e^{-i\vec{q}\cdot\vec{r}}\, n(\vec{r})\, d^3\vec{r} \propto F[n](\vec{q}) = \tilde{n}(\vec{q}).$$

Here $\tilde{n}(\vec{q})$ indicates the 3D Fourier transform of the number density of scatterers $n(\vec{r})$. $\vec{q} = \vec{k}' - \vec{k}$ is the wave vector transferred from the radiation to the sample. Depending on whether the scattering experiment involves X rays or neutrons, $n(\vec{r})$ is the number density of electrons or the number density of nuclear matter, respectively.

The number density of scatterers is

$$(2) \qquad n(\vec{r}) = \sum_{\vec{R}} n_{\text{cell}}(\vec{r} - \vec{R}) \simeq \sum_{\vec{R}} \sum_{s} n_s^{\text{at}}(\vec{r} - \vec{d}_s - \vec{R}),$$

where $\vec{R}$ are the N_{cell} Bravais-lattice translation of a finite piece of a crystal, and $\vec{d}_s$ are the positions of the individual atoms in one primitive cell (the *basis*). The function $n_s^{\text{at}}(\vec{r})$ is the density of the s-th atom in the basis. Depending on whether the experiment is Xray or neutron scattering, $n_s^{\text{at}}(\vec{r})$ is the number density of electrons or the number density of nuclear matter, respectively. The last expression in Eq. (2) is actually exact for the nuclear matter case (neutron scattering). In contrast, the density distribution of electrons in crystals is only approximately the sum of atomic densities, which explains the $\simeq$ sign.

Substitute Eq. (2) into Eq. (1):

$$\begin{aligned}
\tilde{n}(\vec{q}) &= \int_V e^{-i\vec{q}\cdot\vec{r}}\, n(\vec{r})\, d^3\vec{r} = \sum_{\vec{R}} \sum_s \int_V n_s^{\mathrm{at}}(\vec{r} - \vec{d}_s - \vec{R})\, e^{-i\vec{q}\cdot\vec{r}}\, d^3\vec{r} \\
&= \sum_{\vec{R}} \sum_s \int_V n_s^{\mathrm{at}}(\vec{r}\,') \, e^{-i\vec{q}\cdot(\vec{r}\,'+\vec{d}_s+\vec{R})}\, d^3\vec{r}\,' \\
&= \sum_{\vec{R}} e^{-i\vec{q}\cdot\vec{R}} \sum_s e^{-i\vec{q}\cdot\vec{d}_s} \int_V n_s^{\mathrm{at}}(\vec{r}\,') \, e^{-i\vec{q}\cdot\vec{r}\,'}\, d^3\vec{r}\,' \\
&= \sum_{\vec{R}} e^{-i\vec{q}\cdot\vec{R}} \sum_s e^{-i\vec{q}\cdot\vec{d}_s} \int_{\text{all space}} n_s^{\mathrm{at}}(\vec{r}) \, e^{-i\vec{q}\cdot\vec{r}}\, d^3\vec{r} \\
&= \underbrace{\sum_{\vec{R}} e^{-i\vec{q}\cdot\vec{R}}}_{\text{Bragg}} \underbrace{\sum_s e^{-i\vec{q}\cdot\vec{d}_s} f_{\mathrm{at}\,s}(\vec{q})}_{\text{structure factor } S(\vec{q})} \qquad (3)
\end{aligned}$$

Note that the Bravais-lattice sum identified with "Bragg" in the large-sample limit yields the Bragg condition:

$$n_{\mathrm{Bravais}}(\vec{q}) = \sum_{\vec{R}} e^{-i\vec{q}\cdot\vec{R}} \xrightarrow[N_{\mathrm{cell}}\to\infty]{} N_{\mathrm{cell}} \sum_{\vec{G}} \delta_{\vec{q}-\vec{G}} \qquad (4)$$

that directs all scattered amplitude to directions compatible with the Bragg condition

$$\vec{q} = \vec{G}\,. \qquad (5)$$

In Eq. (3) we made use of the observation that $n_s^{\mathrm{at}}(\vec{r})$ is negligibly small for $|\vec{r}| > d$, with d of the order of few nanometers. We have also introduced the *atomic form factor* $f_{\mathrm{at}\,s}(\vec{q})$. Since atoms are spherically symmetric $n_s^{\mathrm{at}}(\vec{r}) = n_s^{\mathrm{at}}(r)$ (the origin is made coincide with the center of the nucleus), the atomic form factor is also spherically symmetric, i.e. it depends only on the length of vector $\vec{q}$. In the simple and "constructive" demonstration below we assume that θ is the angle between vectors $\vec{q}$ and $\vec{r}$:

$$\begin{aligned}
f_{\mathrm{at}\,s}(\vec{q}) &= \int_{\text{all space}} n_s^{\mathrm{at}}(\vec{r})\, e^{-i\vec{q}\cdot\vec{r}}\, d^3\vec{r} \\
&= 2\pi \int_0^\infty r^2\, dr \int_{-1}^{1} d\cos\theta\, n_s^{\mathrm{at}}(r)\, e^{-i\,q\,r\,\cos\theta} \\
&= 2\pi \int_0^\infty r^2\, dr\, n_s^{\mathrm{at}}(r)\, \frac{1}{-i\,q\,r}\left(e^{-i\,q\,r\,1} - e^{-i\,q\,r\,(-1)}\right) \\
&= 4\pi \int_0^\infty n_s^{\mathrm{at}}(r)\, \frac{r}{q} \sin(q\,r)\, dr = f_{\mathrm{at}\,s}(q)\,. \qquad (6)
\end{aligned}$$

Using this result (6), students are invited to solve problem 6 of Kittel's Chapter 2 (evaluation of the atomic form factor of atomic H).

Note that Eq. (6) implies the following observations:

- $f_{\mathrm{at}\,s}(q)$ is a real function;
- for $q \to 0$, $f_{\mathrm{at}\,s}(q) \to f_{\mathrm{at}\,s}(0) = 4\pi \int_0^\infty n_s^{\mathrm{at}}(r)\, r^2\, dr$, the total number of scatterers in a s-labeled atom. For X-ray scattering, this is the number of electrons Z (or slightly more or less if the s atom is ionized). For neutron scattering, $f_{\mathrm{at}\,s}(0)$ reflects the elastic neutron-nucleus cross section at low energy.

In Eq. (3) the quantity identified as the structure factor $S(\vec{q})$ is the only part of the scattering amplitude which is affected by the positions of the atoms in the primitive cell. Note that in the special case of a monoatomic crystal, the $\sum_s$ disappears, and $S(\vec{q}) \equiv f_{\text{at}\,1}(|\vec{q}|)$.

The scattering intensity

$$I(\vec{q}) \propto |\tilde{n}(\vec{q})|^2 = |\tilde{n}_{\text{Bravais}}(\vec{q})|^2 \; |S(\vec{q})|^2 \tag{7}$$

is organized in Bragg peaks at directions uniquely determined by the Bravais lattice of the crystal. In these directions, the scattered intensities are dominated by a common N_{cell}^2 factor from the Bragg term, but are also modulated by the $|S(\vec{q})|^2$ term. From the intensities of the Bragg peaks, crystallographers reconstruct the positions $\vec{d}_s$ of the atoms in the cell. Note however that this reconstruction is not a straightforward inversion of the Fourier transform, because (i) just a finite number of amplitudes $\left|S(\vec{G})\right|$ can be derived from the experimental intensities, at $\vec{q} = \vec{G}$ only, and (ii) no experimental information of the *phase* of the complex structure factor $S(\vec{q})$ is available. In practice crystallographers start from a first guess of the positions $\vec{d}_s$, followed by their iterative adjustments to tune the corresponding $S(\vec{q})$ in order to best fit the experimental scattered intensities.

1.3.1. A note on radiation coherence. What is N_{cell} mentioned below Eq. (2) and in Eq. (4)?

Formally, the number of cells in the crystal.

In practice, the answer is not so straightforward.

The derivation linking the scattered amplitude to the Fourier transform of the density works in the assumptions of:

- a periodic crystal, whose only deviation from ideality is in consisting of a finite number N_{cell} of primitive cells;
- perfect plane-wave incident radiation.

The first assumption is practically valid for a perfect monocrystalline sample. It is certainly violated by polycrystalline materials or powder samples. In those cases, N_{cell} represents the average number of cells in each microcrystal inside the polycrystal, or in each powder grain.

The second assumption regards the *coherence* of the incident radiation. No real radiation source generates perfect plane waves. Every radiation (or matter, in the case of neutrons) beam is perfect and monochromatic to a certain degree. A width in photon energy reflects a mixture of slightly different wave vectors $\vec{k}$. The corresponding photons are generated with random initial phases, and slightly different random propagation directions. In real space this randomness of the radiation field translates in a wave that can be seen as a distortion of a plane wave. If one could examine a small region in space, the electic field (X rays) or the Schrödinger wave function (neutrons) looks practically indistinguishable from a plane wave corresponding to the dominant $\vec{k}$. However over a more extended region, the wave starts to deform significantly. Eventually at two far-enough points, the relative phase of the oscillating field becomes completely random. Coherence is lost. Waves scattered by portions of matter at such large distance cannot interfere any more. The Fourier analysis cannot be applied, and the intensity (rather than the amplitude) of the scattered waves simply sum at the detector. This is what happens when two lamps are turned on at two spots in a room: no coherence, no interference, just the sum of the radiation intensities. The X-rays and neutron beams used in diffractometry are tailored in such a way to produce a radiation as monochromatic and as coherent as possible, but eventually they only provide a finite (and not especially large) *coherence volume* V_{coher}, inside which relative phases are locked and the fields behave as plane waves to a very good approximation.

Given this practical experimental condition, it is clear that N_{cell} cannot exceed V_{coher}/V_c where V_c is the volume of a primitive cell of the crystal under investigation. Therefore in practice the correct value of N_{cell} entering the theorical relations discussed above is the smaller between the average number

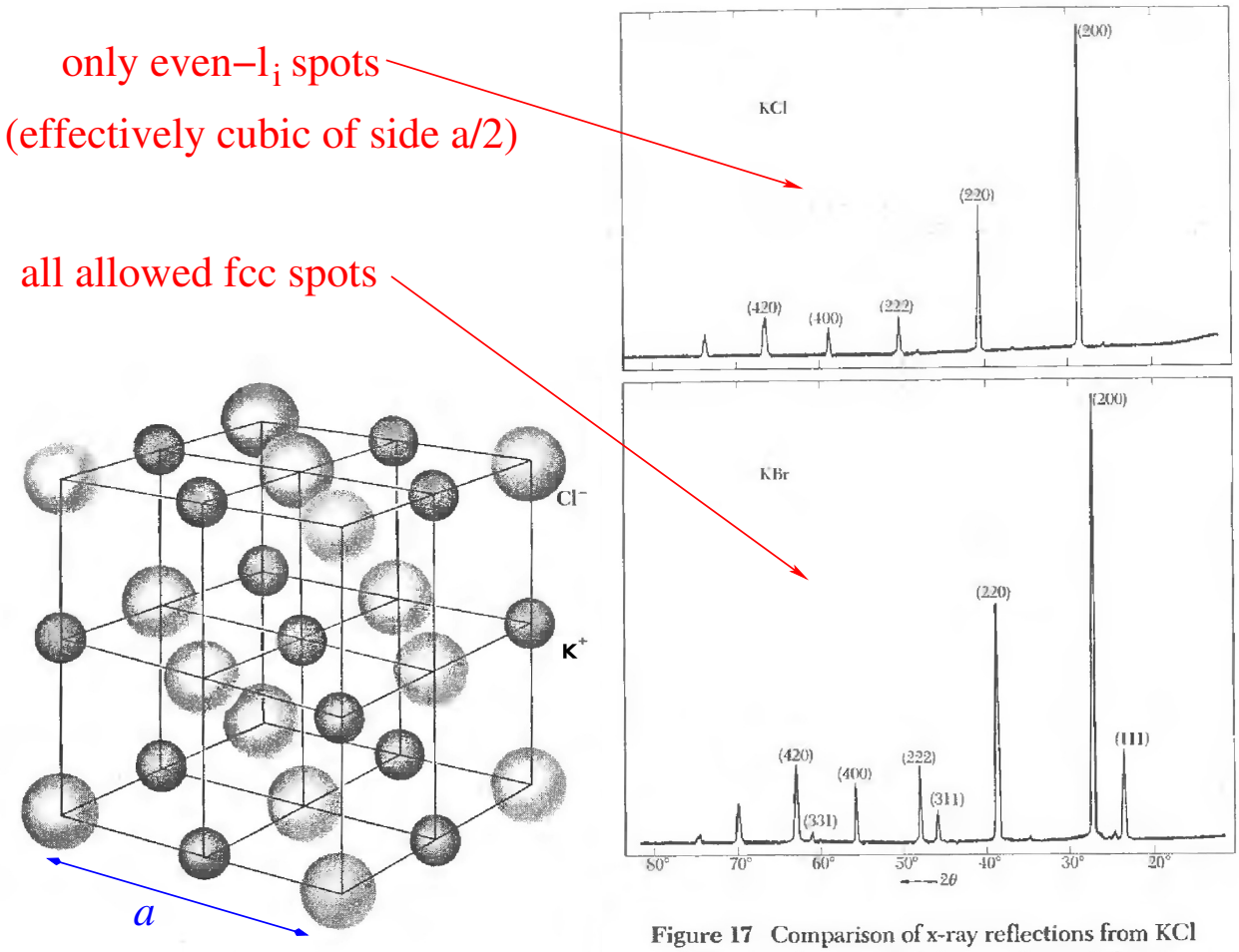

Figure 17 We may construct the sodium chloride crystal structure by arranging K^+ and Cl^- ions alternately at the lattice points of a simple cubic lattice. In the crystal each ion is surrounded by six nearest neighbors of the opposite charge. The space lattice is fcc, and the basis has one Cl^- ion at 000 and one K^+ ion at $\frac{1}{2}\frac{1}{2}\frac{1}{2}$. The figure shows one conventional cubic cell. The ionic diameters here are reduced in relation to the cell in order to clarify the spatial arrangement.

Figure 17 Comparison of x-ray reflections from KCl and KBr powders. In KCl the numbers of electrons of K^+ and Cl^- ions are equal. The scattering amplitudes $f(K^+)$ and $f(Cl^-)$ are almost exactly equal, so that the crystal looks to x-rays as if it were a monatomic simple cubic lattice of lattice constant $a/2$. Only even integers occur in the reflection indices when these are based on a cubic lattice of lattice constant a. In KBr the form factor of Br^- is quite different than that of K^+, and all reflections of the fcc lattice are present. (Courtesy of R. van Nordstrand.)

FIGURE 1.8. Compared powder diffraction peaks of KCl and KBr. Note that the Miller indexes are given relative to the conventional cubic cell of side a

of cells in each (micro)crystal/grain and the number V_{coher}/V_c or unit cells in a radiation coherence volume.

CHAPTER 2

The adiabatic potential and the vibrational dynamics

2.1. The adiabatic separation

For a crystal, as for any piece of matter, the Hamiltonian operator of the system is:

$$\hat{H} = \hat{T}_n + \hat{T}_e + \hat{V}_{ee} + \hat{V}_{en} + \hat{V}_{nn} \tag{8}$$

with:

$$\hat{T}_n = -\frac{\hbar^2}{2}\sum_{i=1}^{N_n}\frac{\Delta_{\vec{R}_i}}{M_i} \quad \text{kinetic energy of the nuclei}$$

$$\hat{T}_e = -\frac{\hbar^2}{2m_e}\sum_{i=1}^{N_e}\Delta_{\vec{r}_i} \quad \text{kinetic energy of the electrons}$$

$$\hat{V}_{ee} = \frac{e^2}{2}\sum_{i\neq j=1}^{N_e}\frac{1}{|\vec{r}_i - \vec{r}_j|} \quad \text{electron-electron repulsion energy}$$

$$\hat{V}_{nn} = \frac{e^2}{2}\sum_{i\neq j=1}^{N_n}\frac{Z_i Z_j}{|\vec{R}_i - \vec{R}_j|} \quad \text{nuclei-nuclei repulsion energy}$$

$$\hat{V}_{en} = -e^2\sum_{i=1}^{N_e}\sum_{j=1}^{N_n}\frac{Z_j}{|\vec{r}_i - \vec{R}_j|} \quad \text{electron-nuclei attraction energy}$$

where e^2 is a shorthand for $q_e^2/(4\pi\epsilon_0)$. Solution of the full eigenvalue equation:

$$\hat{H}\,\Psi(r,R) = E\,\Psi(r,R) \tag{9}$$

would lead to complete knowledge of the properties of the system. As a first step, one could fix a configuration R of the nuclei and focus on the electronic eigenvalue equation:

$$\hat{H}_e^{(R)}\,\Psi^{(e)}(r,R) = V_{\mathrm{ad}}(R)\,\Psi^{(e)}(r,R) \tag{10}$$

where

$$\hat{H}_e^{(R)} = \hat{T}_e + \hat{V}_{ee} + \hat{V}_{en}^{(R)} + \hat{V}_{nn}^{(R)} \tag{11}$$

is the electronic Hamiltonian and $\Psi^{(e)}(r,R)$ is a candidate electronic eigenfunction. Both $\hat{H}_e^{(R)}$ and $\Psi^{(e)}(r,R)$ depend parametrically on the nuclear configuration R. The solution of (10) is complicated by the interaction term $\hat{V}_{ee}$. For the moment, suppose that one could obtain an orthonormal complete set of electronic eigenfunctions:

$$\hat{H}_e^{(R)}\,\Psi_k^{(e)}(r,R) = V_{\mathrm{ad}\,k}(R)\,\Psi_k^{(e)}(r,R)\,. \tag{12}$$

And that this task can be accomplished for every nuclear configuration R. Then, since for every fixed nuclear configuration R a generic electronic wavefunction $\Psi^{(e)}(r,R)$ lies in a space spanned by the

eigenfunctions of Eq. (12), we can expand the total:

$$\Psi(r,R) = \sum_k \Phi_k(R)\,\Psi_k^{(e)}(r,R) \tag{13}$$

The decomposition (13) holds for a generic wavefunction $\Psi(r,R)$, which solves the global eigenvalue problem (9) if and only if the functions $\Phi_k(R)$ satisfy the conditions, which can be obtained by substituting the expansion (13) into Eq. (9):

$$\sum_k \left(\hat{T}_n + \hat{H}_e^{(R)} - E\right)\,\left[\Phi_k(R)\,\Psi_k^{(e)}(r,R)\right] = 0\,. \tag{14}$$

Recalling (12) and the well-known property of the Laplacian operator:

$$\Delta(fg) = (\Delta f)\,g + 2\,(\nabla f)\cdot(\nabla g) + f\,(\Delta g) \tag{15}$$

we rewrite Eq. (14) as

$$\begin{aligned}&\sum_k \left(\hat{T}_n + V_{\mathrm{ad}\,k}(R) - E\right)\,\left[\Phi_k(R)\right]\Psi_k^{(e)}(r,R) + \\ &-\frac{\hbar^2}{2}\sum_k \Phi_k(R)\,\Delta_R\Psi_k^{(e)}(r,R) - \hbar^2\sum_k\left[\nabla_R\Psi_k^{(e)}(r,R)\right]\cdot\nabla_R\left[\Phi_k(R)\right] = 0\,.\end{aligned} \tag{16}$$

where we introduced the shorthand ∇_R, a $3N_n$-dimensional weighted gradient $(\nabla_R)_{j\alpha} \equiv M_j^{-1/2}\left(\vec{\nabla}_{R_j}\right)_\alpha$. and the corresponding Laplacian $\Delta_R \equiv \nabla_R^2$. Taking the inner product with a given electronic eigenfunction $\Psi_l^{(e)}(r,R)$:

$$\begin{aligned}&\left[\hat{T}_n + V_{\mathrm{ad}\,l}(R) - E\right]\,\Phi_l(R) + \\ &-\frac{\hbar^2}{2M}\sum_k \tau_{lk}^{(2)}(R)\,\Phi_k(R) - \frac{\hbar^2}{M}\sum_k \tau_{lk}^{(1)}\cdot\nabla_R\,\Phi_k(R) = 0\end{aligned} \tag{17}$$

where

$$\begin{aligned}\tau_{lk}^{(2)}(R) &= \int dr\,\Psi_l^{(e)*}(r,R)\Delta_R\Psi_k^{(e)}(r,R) \\ \tau_{lk}^{(1)}(R) &= \int dr\,\Psi_l^{(e)*}(r,R)\nabla_R\Psi_k^{(e)}(r,R)\end{aligned} \tag{18}$$

The off-diagonal matrix elements of $\tau^{(2)}$ and $\tau^{(1)}$ are responsible for the couplings between different electronic states l and k.

2.1.1. The adiabatic approximation. The adiabatic approximation implies neglecting precisely the non-adiabatic terms in the lower row of equation (17). When we neglect them, the different electronic states drive the nuclear dynamics "one at a time". At this point, one can fix an electronic eigenstate l (usually the electronic ground state), and obtain the nuclear wave function $\Phi_l(R)$ which is an eigenfunction of the operator

$$\hat{T}_n + V_{\mathrm{ad}\,l}(R)\,.$$

Compared to the general Eq. (13), in the adiabatic approximation the overall eigenfunction $\Psi(r,R)$ involves a single electronic wavefunction:

$$\Psi(r,R) = \Phi_l(R)\,\Psi_l^{(e)}(r,R)\,. \tag{19}$$

This is a wonderful simplification, which allows us to consider the electronic motion to follow "adiabatically" the instantaneous positions R of the nuclei, without worrying of the mixing of different

electronic states. Those who worry that these couplings and mixings might be relevant can always solve the full Eq. (17) taking them into account.

Here we rather address the problem of obtaining $V_{\mathrm{ad}\,l}(R)$, which is the fundamental ingredient driving the motion of the nuclei. Determining $V_{\mathrm{ad}\,l}(R)$ requires solving the electronic equation (10). Due to the electron-electron interaction, this is a rather formidable problem, which can be solved exactly only in remarkably few very ideal conditions, none of which relevant for solids. We will describe approximate approaches to this problem: the Hartree-Fock method and the density-functional theory. In this chapter we focus on the total adiabatic energy $V_{\mathrm{ad}\,l}(R)$ and its implications for the motion of nuclei. We will then come back later on to the electronic implications of the solutions for the electrons.

2.2. The many-electron problem

Recall that the electronic equation, at fixed R involves the following 4 terms:

$$\hat{H}_e^{(R)} = \hat{T}_e + \hat{V}_{en}^{(R)} + \hat{V}_{nn}^{(R)} + \hat{V}_{ee} \,. \tag{20}$$

The electronic problem can be seen as a system of N_e interacting electrons subject to some "external" field. In practice this external field is the Coulomb attraction $\hat{V}_{en}^{(R)}$ due to the N_n nuclei, plus the constant $\hat{V}_{nn}^{(R)}$. Seen from an electron at position $\vec{r}$ this external attraction energy is the following function:

$$V_{\mathrm{ext}}(\vec{r}) = -e^2 \sum_{j=1}^{N_n} \frac{Z_j}{|\vec{r} - \vec{R}_j|} + \frac{e^2}{2} \sum_{i \neq j=1}^{N_n} \frac{Z_i Z_j}{|\vec{R}_i - \vec{R}_j|} \,. \tag{21}$$

From the point of view of the electronic equation, the term $\hat{V}_{nn}^{(R)}$ is a trivial constant: it is a huge positive energy, which however does not influence the motion of the electrons, so we will temporarily set it aside. The electron-electron Coulomb repulsion $\hat{V}_{ee}$ is precisely the responsible for the electronic correlations which make the electronic problem complicate, and call for approximations.

In the following for each electron we introduce a position-spin cumulative coordinate: $w_j = (\vec{r}_j, \sigma_j)$.

If there was no e-e interaction term $\hat{V}_{ee}$, the eigenfunctions of $\hat{H}_e^{(R)}$ would be Slater determinants of the form:

$$\Psi^{(e)}(w_1 \dots w_{N_e}) = \frac{1}{\sqrt{N_e!}} \begin{vmatrix} \phi_1(w_1) & \dots & \phi_{N_e}(w_1) \\ \dots & \dots & \dots \\ \phi_1(w_{N_e}) & \dots & \phi_{N_e}(w_{N_e}) \end{vmatrix} . \tag{22}$$

The single-particle orbitals $\phi_i(w)$ can be, e.g. eigenfunctions of the single-particle Hamiltonian

$$\hat{H}_{0\,j} = -\frac{\hbar^2}{2m_e} \Delta_{\vec{r}_j} + V_{\mathrm{ext}}(\vec{r}_j) \,. \tag{23}$$

Currently, to address the many body-electronic problem there are two main classes of techniques:

- Single-electron methods: Hartree-Fock (HF) and (most approximate) density-functional theory (DFT) variants.
- Intrinsically many-body methods: configuration interaction (CI) and Monte Carlo (MC).

In the following, we briefly review the single-electron methods.

2.3. The Hartree-Fock method

The HF theory moves from the assumption that the ground-state wave function of the interacting electron system can be approximated with a Slater determinant, Eq. (22), constructed with suitably optimized single-particle orbitals.

To identify the best approximation for the actual ground-state wave function in the class of Slater determinants, it is necessary to express the expectation value of $\hat{H}_e^{(R)}$ on $\Psi^{(e)}(w_1 \dots w_{N_e})$ and to minimize it with respect to the involved functions ϕ_i. It is convenient to assume that the single-electron states ϕ_i are orthonormal. All of the (infinitely many) ϕ_i's form a complete set (i.e. a basis) for the one-electron Hilbert space. N_e of them, typically those with the N_e lowest single-electron energies, are involved in the formation of the Slater determinant.

The quantity that we need to optimize is the following average electronic energy:

$$E_{\rm var} = \langle \Psi^{(e)} | \hat{H}_e^{(R)} | \Psi^{(e)} \rangle = \int dw_1 \dots dw_{N_e} \Psi^{(e)*}(w_1 \dots w_{N_e}) \hat{H}_e^{(R)} \Psi^{(e)}(w_1 \dots w_{N_e}), \tag{24}$$

with the natural notation $\int dw_j \equiv \int d^3\vec{r}_j \sum_{\sigma_j}$.

$E_{\rm var}$ is the sum of the quantum averages of two operators: a 1-electron operator $O^{(1)}$, namely

$$\hat{H}_0 = \sum_{j=1}^{N_e} \hat{H}_{0\,j}\,, \tag{25}$$

– see Eq. (23), plus a 2-electron operator $O^{(2)}$, namely

$$\hat{V}_{ee} = \frac{1}{2} \sum_{j=1}^{N_e} \sum_{j' \neq j} \hat{V}_{{\rm C}\,j,j'}\,. \tag{26}$$

Here the Coulomb 2-body interaction between electrons j and j' is

$$\hat{V}_{{\rm C}\,j,j'} = \frac{e^2}{|\vec{r}_j - \vec{r}_{j'}|}\, \mathbb{1}_{{\rm spin}\,j}\, \mathbb{1}_{{\rm spin}\,j'}\,, \tag{27}$$

where $\mathbb{1}_{{\rm spin}\,l}$ is the identity in the spin space of the l-th electron. This identity, sometimes left implicit, is due to the Coulomb repulsion being an orbital operator, not affecting the electrons' spins.

We will find that the 1-electron operator generates N_e individual contributions $\langle \phi_i | \hat{H}_0 | \phi_i \rangle$; the 2-electron operator generates N_e^2 contributions. Let us compute the two terms separately.

For the $O^{(1)}$:

$$\begin{aligned}
\langle \Psi^{(e)} | O^{(1)} | \Psi^{(e)} \rangle &= \frac{1}{N_e!} \sum_P \sum_{P'} (-1)^{P+P'} \sum_j \langle \phi_{P_1} | \phi_{P'_1} \rangle \langle \phi_{P_2} | \phi_{P'_2} \rangle \dots \langle \phi_{P_j} | O_j^{(1)} | \phi_{P'_j} \rangle \dots \langle \phi_{P_{N_e}} | \phi_{P'_{N_e}} \rangle \\
&= \frac{1}{N_e!} \sum_P \sum_{P'} (-1)^{P+P'} \sum_j \delta_{P_1,P'_1}\, \delta_{P_2,P'_2} \dots \langle \phi_{P_j} | O_j^{(1)} | \phi_{P'_j} \rangle \dots \delta_{P_{N_e},P'_{N_e}} \\
&= \frac{1}{N_e!} \sum_P \sum_j \langle \phi_{P_j} | O_j^{(1)} | \phi_{P_j} \rangle = \frac{1}{N_e} \sum_{l=1}^{N_e} \sum_j \langle \phi_l | O_j^{(1)} | \phi_l \rangle = \sum_{l=1}^{N_e} \langle \phi_l | O_1^{(1)} | \phi_l \rangle\,.
\end{aligned} \tag{28}$$

Here we used

- the orthornormality of the set of single-electron wavefunctions $\langle \phi_k | \phi_{k'} \rangle = \delta_{kk'}$;
- the fact that two permutations P and P' with $N_e - 1$ equal indexes must necessarily coincide;
- the fact that the $(N_e - 1)!$ permutations of the indexes different from j do not affect the summed quantity;
- the possibility to re-name the permutated index $l \equiv P_j$, which just takes the values $1 \dots N_e$;
- the fact that the index j just labels a mute integration variable: the results of the integration do not depend on whether we call that variable w_1 or w_2 or any other of them.

The conclusion of this calculation is that the average value of any $O^{(1)}$ operator on a Slater determinant is just the sum of the averages of the operator itself on the N_e single-particle states composing the Slater determinant.

Let us proceed to the average of $O^{(2)}$:

$$\begin{aligned}
\langle\Psi^{(e)}|O^{(2)}|\Psi^{(e)}\rangle =& \frac{1}{N_e!}\sum_P\sum_{P'}(-1)^{P+P'}\frac{1}{2}\sum_j\sum_{j'\neq j} \\
& \underbrace{\langle\phi_{P_1}|\phi_{P'_1}\rangle}_{\delta_{P_1,P'_1}}\underbrace{\dots}_{\text{no } j,j'}\underbrace{\langle\phi_{P_{N_e}}|\phi_{P'_{N_e}}\rangle}_{\delta_{P_{N_e},P'_{N_e}}}\langle\phi_{P_j}|\langle\phi_{P_{j'}}|O^{(2)}_{jj'}|\phi_{P'_j}\rangle|\phi_{P'_{j'}}\rangle \\
=& \frac{1}{N_e!}\sum_P\frac{1}{2}\sum_j\sum_{j'\neq j}\left(\langle\phi_{P_j}|\langle\phi_{P_{j'}}|O^{(2)}_{jj'}|\phi_{P_j}\rangle|\phi_{P_{j'}}\rangle - \langle\phi_{P_j}|\langle\phi_{P_{j'}}|O^{(2)}_{jj'}|\phi_{P_{j'}}\rangle|\phi_{P_j}\rangle\right) \\
=& \frac{1}{N_e(N_e-1)}\sum_l\sum_{l'\neq l}\frac{1}{2}\sum_j\sum_{j'\neq j}\left(\langle\phi_l|\langle\phi_{l'}|O^{(2)}_{jj'}|\phi_l\rangle|\phi_{l'}\rangle - \langle\phi_l|\langle\phi_{l'}|O^{(2)}_{jj'}|\phi_{l'}\rangle|\phi_l\rangle\right) \\
=& \frac{1}{2}\sum_l\sum_{l'\neq l}\left(\langle\phi_l|\langle\phi_{l'}|O^{(2)}_{12}|\phi_l\rangle|\phi_{l'}\rangle - \langle\phi_l|\langle\phi_{l'}|O^{(2)}_{12}|\phi_{l'}\rangle|\phi_l\rangle\right) \\
=& \frac{1}{2}\sum_l\sum_{l'}\left(\langle\phi_l|\langle\phi_{l'}|O^{(2)}_{12}|\phi_l\rangle|\phi_{l'}\rangle - \langle\phi_l|\langle\phi_{l'}|O^{(2)}_{12}|\phi_{l'}\rangle|\phi_l\rangle\right).
\end{aligned} \tag{29}$$

Observations:

- we use the orthornormality of the set of single-particle wavefunctions;
- two permutations P and P' with N_e-2 equal indexes either coincide or have the two non-coincident indexes swapped; in the first case the parity sign $(-1)^{P+P'}=1$, in the second case $(-1)^{P+P'}=-1$;
- the $(N_e-2)!$ permutations of the indexes different from j and j' do not affect the summed quantity;
- we re-name the permuted indexes $l\equiv P_j$ $l'\equiv P_{j'}$, which must take different values;
- indexes j and j' just label two mute integration variables w_j and $w_{j'}$: the results of the integration do not depend on the names of these variables;
- the condition $l'\neq l$ can be removed, because its removal adds equal unphysical terms before and after the minus sign. These terms cancel anyway, and the overall result remains the same.

The conclusion of this calculation is that on a a Slater determinant the average value of any $O^{(2)}$ operator involves two terms: a Hartree term

$$\frac{1}{2}\sum_{l,l'}\langle\phi_l|\langle\phi_{l'}|O^{(2)}_{12}|\phi_l\rangle|\phi_{l'}\rangle \tag{30}$$

and a Fock term

$$-\frac{1}{2}\sum_{l,l'}\langle\phi_l|\langle\phi_{l'}|O^{(2)}_{12}|\phi_{l'}\rangle|\phi_l\rangle\,. \tag{31}$$

Each of them involves the summation of N_e^2 terms obtained by applying the two body-operator on all possible pairs resulting from the N_e single-particle states composing the Slater determinant.

We can now use these general results to compute the average energy that the HF method purposes to minimize:

$$\begin{aligned}
E_{\text{var}} &= \langle\Psi^{(e)}|\hat{H}_0|\Psi^{(e)}\rangle + \langle\Psi^{(e)}|\hat{V}_{ee}|\Psi^{(e)}\rangle \\
&= \sum_l\langle\phi_l|\hat{H}_{0\,1}|\phi_l\rangle + \frac{1}{2}\sum_{l,l'}\left(\langle\phi_l|\langle\phi_{l'}|\hat{V}_{\text{C}\,1,2}|\phi_l\rangle|\phi_{l'}\rangle - \langle\phi_l|\langle\phi_{l'}|\hat{V}_{\text{C}\,1,2}|\phi_{l'}\rangle|\phi_l\rangle\right),
\end{aligned} \tag{32}$$

Observations on Eq. (32):

(1) The Coulomb operator in the Hartree term finds the same pair of bras and kets at both sides, in the same order. Therefore, the spin identities $\mathbb{1}_{\text{spin}}$ of Eq. (27) are automatically satisfied there, regardless of the two electrons having the same or different spin wavefunctions.
(2) On the contrary, $\mathbb{1}_{\text{spin}}$ affects the Fock term, setting to 0 all terms which have $\sigma_l \neq \sigma_{l'}$. Accordingly, the more electrons have the same spin component, the more nonvanishing terms the Fock sum has. Since the Fock term is a negative correction to the positive Hartree term, states with several electrons with the same spin component (and accordingly large total spin) have more nonzero Fock terms and are favored energetically against states with better spin compensation. This phenomenon is called *spin exchange*, and it is at the origin of *magnetism* in atoms, molecules, nanoparticles, and solids.

2.3.1. The electron density. Before minimizing Eq. (32), we make a short digression on the electrons density. The density operator is defined as

$$\hat{n}(\vec{r}) = \sum_{j=1}^{N_e} \delta\left(\hat{\vec{r}}_j - \vec{r}\right) \mathbb{1}_{\text{spin } j} \,. \tag{33}$$

Here $\hat{\vec{r}}_j$ is the position operators of electron j. $\vec{r}$ is a fixed (classical) vector in the 3D space, indentifying the place where we wish to measure the number density. The spin identity emphasizes the fact that the density gives purely positional informations.

It is useful to introduce the average of $\hat{n}(\vec{r})$ over the quantum state of the system:

$$n(\vec{r}) = \langle \Psi^{(e)} | \hat{n}(\vec{r}) | \Psi^{(e)} \rangle \,. \tag{34}$$

This average density is usually simply referred to as the "electron density at position $\vec{r}$". $n(\vec{r})$ is a ordinary real function of three variables. Its physical dimension is $[\text{length}]^{-3}$.

Clearly, this density can be computed on any many-body state of N_e electrons.

Now that we are dealing with the HF method, we compute $n(\vec{r})$ for the special case of a Slater-determinant state. The main observation is that $\hat{n}(\vec{r})$ is a one-body operator, as it is clear from its definition (33). Therefore, using the result of Eq. (28):

$$n(\vec{r}) = \sum_k \langle \phi_k | \delta(\hat{\vec{r}}_1 - \vec{r}) | \phi_k \rangle = \sum_k \int d^3\vec{r}_1 \sum_{\sigma_1} \phi_k^*(\vec{r}_1, \sigma_1) \delta(\vec{r}_1 - \vec{r}) \phi_k(\vec{r}_1, \sigma_1) = \sum_k \sum_\sigma |\phi_k(\vec{r}, \sigma)|^2. \tag{35}$$

2.3.2. The variational energy in terms of $n(\vec{r})$. Going back to the HF calculation, two of the terms in the variational energy can be expressed as functions of the density: the interaction with the

external potential, Eq. (21), and the Hartree term:

$$
\begin{aligned}
E_{\text{var}} &= \sum_l \langle\phi_l| -\frac{\hbar^2}{2m_e}\Delta_{\vec{r}}|\phi_l\rangle + \sum_l \sum_\sigma \int d^3\vec{r}_1\, \phi_l^*(\vec{r}_1,\sigma) V_{\text{ext}}(\vec{r}_1)\phi_l(\vec{r}_1,\sigma) \\
&\quad + \frac{1}{2}\sum_{l,l'}\sum_{\sigma_1}\int d^3\vec{r}_1 \sum_{\sigma_2}\int d^3\vec{r}_2\, \phi_l^*(\vec{r}_1,\sigma_1)\phi_{l'}^*(\vec{r}_2,\sigma_2)\hat{V}_{\text{C}\,1,2}\,\phi_l(\vec{r}_1,\sigma_1)\phi_{l'}(\vec{r}_2,\sigma_2) \\
&\quad - \frac{1}{2}\sum_{l,l'} \langle\phi_l|\,\langle\phi_{l'}|\,\hat{V}_{\text{C}\,1,2}\;|\phi_{l'}\rangle\,|\phi_l\rangle \\
&= \sum_l \langle\phi_l| -\frac{\hbar^2}{2m_e}\Delta_{\vec{r}}|\phi_l\rangle + \int d^3\vec{r}_1\, V_{\text{ext}}(\vec{r}_1)\sum_l\sum_\sigma |\phi_l(\vec{r}_1,\sigma)|^2 \\
&\quad + \frac{1}{2}\int d^3\vec{r}_1 \int d^3\vec{r}_2 \sum_l\sum_{\sigma_1} |\phi_l(\vec{r}_1,\sigma_1)|^2\,\hat{V}_{\text{C}\,1,2}\sum_{l'}\sum_{\sigma_2}|\phi_{l'}(\vec{r}_2,\sigma_2)|^2 \\
&\quad - \frac{1}{2}\sum_{l,l'} \langle\phi_l|\,\langle\phi_{l'}|\,\hat{V}_{\text{C}\,1,2}\;|\phi_{l'}\rangle\,|\phi_l\rangle \\
&= \sum_l \langle\phi_l| -\frac{\hbar^2}{2m_e}\Delta_{\vec{r}}|\phi_l\rangle + \int d^3\vec{r}\, V_{\text{ext}}(\vec{r})\, n(\vec{r}) \\
&\quad + \frac{1}{2}\int d^3\vec{r}_1 \int d^3\vec{r}_2\, n(\vec{r}_1)\frac{e^2}{|\vec{r}_1-\vec{r}_2|}n(\vec{r}_2) - \frac{1}{2}\sum_{l,l'}\langle\phi_l|\,\langle\phi_{l'}|\,\hat{V}_{\text{C}\,1,2}\,|\phi_{l'}\rangle\,|\phi_l\rangle \\
&= E_{\text{kin}}[\{\phi_j\}] + E_{\text{ext}}[n] + E_{\text{Hartree}}[n] + E_{\text{x}}[\{\phi_j\}].
\end{aligned}
\tag{36}
$$

Note that in this form the Hartree term exhibits the classic form of the electrostatic repulsion energy of a charge distribution $n(\vec{r})$ with itself. By definition, this is the work needed to pull the "charge elements" from infinitely far apart against the electric forces that repel them, until the charge distribution $n(\vec{r})$ is assembled.

The energy $E_{\text{var}} = \langle\Psi^{(e)}|\hat{H}_e^{(R)}|\Psi^{(e)}\rangle$ must be minimized as a *functional* of the single-particle orbitals ϕ_i. Several techniques have been devised to carry out this minimization. For example one can parameterize the $\{\phi_j\}$ in terms of certain parameters (e.g. the values of the $\phi_j(\vec{r})$ at certain positions in real space), and then minimize E_{var} by adjusting these parameters. Here we will rather discuss a classic formulation of this minimization, in terms of functional derivatives, leading to a differential equation: the Hartree-Fock equation.

2.3.3. Minimization of the variational energy. We address the minimization of E_{var} as a functional problem, by means of a functional differentiation, see Appendix A.

Note the extra complication that during the minimization we must make sure that the single-particle orbitals ϕ_j remain orthonormal. This result can be achieved by means of Lagrange multipliers. The stationary condition for the optimization of E_{var} is:

$$
\frac{\delta}{\delta\phi_k(\vec{r})}\left[\langle\Psi^{(e)}|\hat{H}_e^{(R)}|\Psi^{(e)}\rangle - \sum_{i,j}\lambda_{ij}\left(\langle\phi_i|\phi_j\rangle - \delta_{ij}\right)\right] = 0 \tag{37}
$$

We apply the techniques of functional derivatives. For convenience, we take the derivative of E_{var} with respect to ϕ_k^*, instead of ϕ_k. Two of the terms depend on the wavefunctions through the density n. Given the usual notation $w = (\vec{r},\sigma)$ being the spot where the functional derivative is carried out,

and $w' = (\vec{r}', \sigma')$ being the dummy internal variable, we evaluate

$$\frac{\delta}{\delta\phi_k^*(w)} n(\vec{r}') = \frac{\delta}{\delta\phi_k^*(w)} \sum_j \sum_{\sigma'} \phi_j^*(w')\phi_j(w') = \delta(\vec{r} - \vec{r}')\delta_{\sigma,\sigma'}\phi_k(w') \,. \tag{38}$$

This result allows us to calculate what we really need through the chain rule:

$$\begin{aligned} \frac{\delta}{\delta\phi_k^*(w)}\Phi[n] &= \int d^3\vec{r}' \sum_{\sigma'} \left[\frac{\delta}{\delta n(\vec{r}')}\Phi[n]\right] \frac{\delta n(\vec{r}')}{\delta\phi_k^*(w)} \\ &= \int d^3\vec{r}' \sum_{\sigma'} \frac{\delta\Phi[n]}{\delta n(\vec{r}')}\delta(\vec{r} - \vec{r}')\delta_{\sigma,\sigma'}\phi_k(\vec{r}', \sigma') = \frac{\delta\Phi[n]}{\delta n(\vec{r})}\,\phi_k(w) \,. \end{aligned} \tag{39}$$

This result allows us to determine the contributions of $E_{\rm ext}[n]$ and $E_{\rm Hartree}[n]$.

The external potential gives the simplest derivative:

$$\frac{\delta E_{\rm ext}[n]}{\delta n(\vec{r})} = V_{\rm ext}(\vec{r}) \,, \tag{40}$$

which generates a term

$$\frac{\delta E_{\rm ext}[n]}{\delta\phi_k^*(w)} = V_{\rm ext}(\vec{r})\phi_k(w) \qquad [\text{where } w = (\vec{r}, \sigma)] \tag{41}$$

in the HF equation. This same result could be easily obtained even by carrying out directly the functional derivative of the formulation of $E_{\rm ext}$ in the first line of Eq. (36).

The Hartree term is quadratic in n, therefore

$$\frac{\delta E_{\rm Hartree}[n]}{\delta n(\vec{r})} = \frac{1}{2}\int d^3\vec{r}' \left(\frac{e^2}{|\vec{r} - \vec{r}'|} + \frac{e^2}{|\vec{r}' - \vec{r}|}\right) n(\vec{r}') = \int d^3\vec{r}' \frac{e^2}{|\vec{r} - \vec{r}'|} n(\vec{r}') \,, \tag{42}$$

which provides a term

$$\frac{\delta E_{\rm Hartree}[n]}{\delta\phi_k^*(w)} = \int d^3\vec{r}' \frac{e^2}{|\vec{r} - \vec{r}'|} n(\vec{r}')\,\phi_k(w) \qquad [\text{where } w = (\vec{r}, \sigma)] \tag{43}$$

to the HF equation.

The derivation of the kinetic energy is quite straightforward, too. We do not involve the density at all, and obtain:

$$\begin{aligned} \frac{\delta E_{\rm kin}[\{\phi_j\}]}{\delta\phi_k^*(w)} =& \frac{\delta}{\delta\phi_k^*(w)} \sum_l \langle\phi_l| - \frac{\hbar^2}{2m_e}\Delta_{\vec{r}'}|\phi_l\rangle = \frac{\delta}{\delta\phi_k^*(w)} \langle\phi_k| - \frac{\hbar^2}{2m_e}\Delta_{\vec{r}'}|\phi_k\rangle \\ =& \frac{\delta}{\delta\phi_k^*(w)} \int d^3\vec{r}'\phi_k^*(\vec{r}', \sigma) \left[-\frac{\hbar^2}{2m_e}\Delta_{\vec{r}'}\right] \phi_k(\vec{r}', \sigma) = -\frac{\hbar^2}{2m_e}\Delta_{\vec{r}}\,\phi_k(w) \,, \end{aligned} \tag{44}$$

the kinetic term in the HF equation.

The Fock contribution is the most intricate one. In the double summation, $\phi_k^*(\cdot,\cdot)$, alias $\langle\phi_k|$, appears twice. Therefore two terms arise in the derivative:

$$\begin{aligned}
\frac{\delta E_{\mathrm{x}}[\{\phi_j\}]}{\delta\phi_k^*(w)} =& \frac{\delta}{\delta\phi_k^*(w)}\left[-\frac{1}{2}\sum_{l,l'}\langle\phi_l|\,\langle\phi_{l'}|\,\hat{V}_{\mathrm{C}\,1,2}\,|\phi_{l'}\rangle\,|\phi_l\rangle\right] \\
=& -\frac{1}{2}\frac{\delta}{\delta\phi_k^*(w)}\sum_{l,l'} \\
& \int d\vec{x}_1\int d\vec{x}_2\sum_{\sigma_1\sigma_2}\phi_l^*(\vec{x}_1,\sigma_1)\phi_{l'}^*(\vec{x}_2,\sigma_2)\frac{e^2}{|\vec{x}_1-\vec{x}_2|}\mathbb{1}_{\mathrm{spin}\,1}\,\mathbb{1}_{\mathrm{spin}\,2}\phi_{l'}(\vec{x}_1,\sigma_1)\phi_l(\vec{x}_2,\sigma_2) \\
=& \underbrace{-\frac{1}{2}\sum_{l}\sum_{\sigma_1}\langle\phi_l|\,\frac{e^2}{|\vec{x}_1-\vec{r}|}\mathbb{1}_{\mathrm{spin}\,1}\,|\phi_k\rangle\,\phi_l(w)}_{l'\to k,\ \vec{x}_2\to\vec{r}\ \sigma_2\to\sigma} \\
& \underbrace{-\frac{1}{2}\sum_{l'}\sum_{\sigma_2}\langle\phi_{l'}|\,\frac{e^2}{|\vec{r}-\vec{x}_2|}\mathbb{1}_{\mathrm{spin}\,2}\,|\phi_k\rangle\,\phi_{l'}(w)}_{l\to k,\ \vec{x}_1\to\vec{r}\ \sigma_1\to\sigma} \\
=& -\sum_{l}\sum_{\sigma_1}\phi_l(w)\,\langle\phi_l|\,\frac{e^2}{|\vec{r}-\vec{x}_1|}\mathbb{1}_{\mathrm{spin}\,1}\,|\phi_k\rangle\,, \qquad (45)
\end{aligned}$$

where, as above, $w = (\vec{r},\sigma)$. The two terms obtained through derivation are the same, just with different names of dummy summation and integration variables. Thus, in the last line we drop the $1/2$ factor and keep only one term. In the common situation where the HF single-electron kets are eigenkets of S_z, the spin identity in the Fock term generates a Kroneker $\delta_{\sigma_1,\sigma_k}$, thus practically removing the summation over σ_1 (leaving only a spatial integration over $\vec{x}_1$). As a consequence, of all N_e states in the l sum, those with spin projection orthogonal to that of electron k do not contribute to the Fock term.

Finally, the Lagrange-multipler term yields:

$$\frac{\delta}{\delta\phi_k^*(w)}\sum_{ij}\lambda_{ij}\left(\langle\phi_i|\phi_j\rangle-\delta_{ij}\right) = \sum_j\lambda_{kj}\phi_j(w)\,. \qquad (46)$$

The matrix λ_{ij} of Lagrange multipliers is real-valued and symmetric. Without loss of generality, we can suppose we make a unitary transformation in the N_n-dimensional space span by the $|\phi_i\rangle$, such that the matrix of the λ_{ij} coefficient becomes diagonal. With this assumption $\lambda_{ij} = \delta_{ij}\epsilon_i$.

Now we combine these 5 terms to obtain the Hartree-Fock equation:

$$\begin{aligned}
-\frac{\hbar^2}{2m_e}\Delta_{\vec{r}}\,\phi_k(w) + V_{\mathrm{ext}}(\vec{r})\phi_k(w) + \int d^3\vec{r}\,'\frac{e^2}{|\vec{r}-\vec{r}\,'|}n(\vec{r}\,')\,\phi_k(w) + \\
- \sum_l\phi_l(w)\,\langle\phi_l|\,\frac{e^2}{|\vec{r}-\vec{x}_1|}\mathbb{1}_{\mathrm{spin}\,1}\,|\phi_k\rangle = \epsilon_k\phi_k(w)\,. \qquad (47)
\end{aligned}$$

This HF equation is a nonlinear equation for the single-electron orbitals. However, one can attempt to view it as a linear equation, if one focuses on $\phi_k(\vec{r})$. In this linearized picture, the Hartree and Fock terms of Eq. (47) depend explicitly on the (yet unknown) wavefunctions ϕ_l. A standard strategy for the solution of the HF equation is based on repeatedly pretending that all ϕ_l – and correspondingly the density $n(\vec{r})$ – in Eq. (47) are known. One starts from some arbitrary initial set of N_e orthonormal one-electron wavefunctions, puts them in place of all ϕ_l's in Eq. (47), thus generating a first approximation

for the effective potential energy acting on the single electrons; solves (usually numerically) the linear equation for ϕ_k; from the list of solutions, takes the N_e eigenfunctions with lowest *single-particle eigenenergy* ϵ_k (*aufbau* rule); re-inserts them into Eq. (47) in place of the ϕ_l's thus generating a better approximation for the effective potential energy; iterates this procedure until convergence. After several iterations ($\approx 10 \div 100$, depending on the starting ψ_β), *self-consistency* is usually reached, i.e. the wavefunctions do not change appreciably from one iteration to the next. This is usually done numerically, by expanding the one-electron orbitals on a fixed basis, and solving self-consistently the equation for the expansion coefficients.

Electrons described by a Slater determinant are subjected to the external potential, to an electrostatic-like mean-field potential (the Hartree term), plus a further *non-local* potential (the Fock exchange term) due to the antisymmetric structure of the wavefunction, related to Pauli's exclusion principle. The non-locality refers to $\phi_k(w')$ appearing in this term inside an integral over all positions, not just at w as in all other appearances of $\phi_k(\ )$ in the HF equation.

Many of the discussed properties apply to Kohn-Sham density functional theory, too. As we see below, this theory bears a formal resemblance to Hartree-Fock theory, despite being conceptually different.

Once the self-consistent problem is solved, the single-electron orbitals $|\phi_k\rangle$ can be plugged in into Eq. (22). to construct the HF ground state. They can also be substituted into Eq. (36), to determine the HF approximation to the GS energy: $E_{\rm HF} = \min E_{\rm var}$. Note that $E_{\rm HF} \neq \sum_k \epsilon_k$.

Observe that the HF equation targets a *stationary state*, not necessarily the ground state. This means that it can in principle be used even to compute electronically excited states.

It is possible to improve systematically the accuracy of this many-body theory, by going beyond the Hartree-Fock single-determinant approximation. The standard method pursuing this project is called *configuration interaction* (CI) approach, in which the ground-state electronic wavefunction is expressed as a *linear combination* of several Slater determinants, rather than just one. However this approach is rarely carried out for solids.

2.4. Density-Functional Theory

The *density functional theory* (DFT) [**5**] approach to the calculation of ground-state properties of a many-electron system, relies on the crucial observation, due to Hohenberg and Köhn, that the ground-state density

$$n_0(\vec{r}) = \langle \Psi_0^{(e)} | \hat{n}(\vec{r}) | \Psi_0^{(e)} \rangle \,,$$

see Eq. (34), provides sufficient information to calculate all other ground-state properties.

2.4.1. The Hohenberg-Kohn Theorems (1965). In rigorous terms, the Hohenberg-Kohn Theorem states that the GS energy of an interacting N_e-particle system can be computed as a functional of the GS density $n_0(\vec{r})$. This is a surprising and counterintuitive result, as the mapping $|\Psi^{(e)}\rangle \to n$ is obviously *not injective*: there are infinitely many many-body wavefunctions that produce the same average density. We will prove this result under the simplifying assumption that the GS of the electronic system is non-degenerate.

2.4.1.1. *The First Theorem.* If the two-body interaction is fixed, the mapping:

$$V_{\rm ext}(\vec{r}) \to |\Psi_0^{(e)}\rangle \to n_0(\vec{r}) \tag{48}$$

is a bijection, up to a constant shift in $V_{\rm ext}$.

Proof.

The fact that this mapping is surjective can always be guaranteed by suitably defining the space of acceptable GS kets $|\Psi_0^{(e)}\rangle$ and the space of acceptable GS densities $n_0(\vec{r})$. We just need to prove that both steps of this mapping are injective, i.e. that different (not just by a constant) external potentials lead to different GS densities.

Fix two external potentials V_{ext} and V'_{ext} which differ more substantially than just by a constant. Then, the two Hamiltonian operators:

$$\hat{H}_e^{(R)} = \hat{T}_e + \hat{V}_{ee} + \hat{V}_{\text{ext}} \tag{49}$$

$$\hat{H}_e^{(R)'} = \hat{T}_e + \hat{V}_{ee} + \hat{V}'_{\text{ext}} \tag{50}$$

give rise to ground states $|\Psi_0^{(e)}\rangle$ and $|\Psi_0^{(e)'}\rangle$ respectively.

Assume, *ad absurdum*, that $|\Psi_0^{(e)}\rangle = |\Psi_0^{(e)'}\rangle$, then:

$$(\hat{H}_e^{(R)} - \hat{H}_e^{(R)'})\,|\Psi_0^{(e)}\rangle = (E_0 - E'_0)\,|\Psi_0^{(e)}\rangle\ , \tag{51}$$

i.e.

$$(\hat{V}_{\text{ext}} - \hat{V}'_{\text{ext}})\,|\Psi_0^{(e)}\rangle = (E_0 - E'_0)\,|\Psi_0^{(e)}\rangle\ . \tag{52}$$

Since $\hat{V}_{\text{ext}}$ and $\hat{V}'_{\text{ext}}$ are multiplicative 1-body operators:

$$\hat{V}_{\text{ext}} - \hat{V}'_{\text{ext}} = E_0 - E'_0\,, \tag{53}$$

i.e.

$$V_{\text{ext}}(\vec{r}) - V'_{\text{ext}}(\vec{r}) = E_0 - E'_0 \tag{54}$$

almost everywhere: the two potentials differ by a constant energy, which negates the hypothesis. We conclude that:

$$|\Psi_0^{(e)}\rangle = |\Psi_0^{(e)'}\rangle \iff V_{\text{ext}} = V'_{\text{ext}} + \text{const} \tag{55}$$

In other words, the external potential fixes univocally the GS wavefunction, and viceversa. There do not exist two really different V_{ext}'s that lead to the same GS wavefunction.

To prove the second step, we first recall that starting from a many-body wavefunction, evaluating the average density is straightforward, following the definition Eq. (34):

$$\begin{aligned}
n(\vec{r}) &= \langle\Psi^{(e)}|\hat{n}(\vec{r})|\Psi^{(e)}\rangle = \langle\Psi^{(e)}|\sum_j \delta(\hat{\vec{r}}_j - \vec{r})|\Psi^{(e)}\rangle = \sum_j \langle\Psi^{(e)}|\delta(\hat{\vec{r}}_j - \vec{r})|\Psi^{(e)}\rangle \\
&= \langle\Psi^{(e)}|\delta(\hat{\vec{r}}_1 - \vec{r})|\Psi^{(e)}\rangle + \langle\Psi^{(e)}|\delta(\hat{\vec{r}}_2 - \vec{r})|\Psi^{(e)}\rangle + \ldots\ [N_e - 2 \text{ similar terms}] \\
&= \sum_{\sigma_1}\int dw_2 \int dw_3 \cdots \int dw_{N_e} \left|\Psi^{(e)}(\vec{r}\,\sigma_1, w_2, w_3, \ldots, w_{N_e})\right|^2 + \\
&+ \int dw_1 \sum_{\sigma_2}\int dw_3 \cdots \int dw_{N_e} \left|\Psi^{(e)}(w_1, \vec{r}\,\sigma_2, w_3, \ldots, w_{N_e})\right|^2 + \ldots \\
&= N_e \sum_{\sigma_1}\int dw_2 \int dw_3 \cdots \int dw_{N_e} \left|\Psi^{(e)}(\vec{r}\,\sigma_1, w_2, w_3, \ldots, w_{N_e})\right|^2 .
\end{aligned} \tag{56}$$

The last step is a consequence of the many-body wavefunction of identical fermions being totally antisymmetric under the exchange of any two of its arguments w_l. In practice, given a many-body wavefunction, to obtain the corresponding density one simply integrates its square modulus over $N_e - 1$ position variables, with the remaining one fixed to $\vec{r}$, and sums over all N_e spin components.

To complete the proof, assume now $|\Psi_0^{(e)}\rangle \neq |\Psi_0^{(e)'}\rangle$. Use the obvious $\hat{H}_e^{(R)} = \hat{H}_e^{(R)'} + \hat{V}_{\text{ext}} - \hat{V}'_{\text{ext}}$, and apply Ritz's variational principle:

$$E_0 = \langle\Psi_0^{(e)}|\hat{H}_e^{(R)}|\Psi_0^{(e)}\rangle < \langle\Psi_0^{(e)'}|\hat{H}_e^{(R)}|\Psi_0^{(e)'}\rangle = E'_0 + \langle\Psi_0^{(e)'}|\hat{V}_{\text{ext}} - \hat{V}'_{\text{ext}}|\Psi_0^{(e)'}\rangle\,. \tag{57}$$

Therefore:

$$E_0 - E'_0 < \int d^3\vec{r}\,\left(V_{\text{ext}}(\vec{r}) - V'_{\text{ext}}(\vec{r})\right) n'_0(\vec{r})\,. \tag{58}$$

In a similar fashion, using $\hat{H}_e^{(R)'} = \hat{H}_e^{(R)} + \hat{V}'_{\rm ext} - \hat{V}_{\rm ext}$:

$$E'_0 - E_0 < \int d^3\vec{r}\,\left(V'_{\rm ext}(\vec{r}) - V_{\rm ext}(\vec{r})\right) n_0(\vec{r}). \tag{59}$$

Summing these relations leads to

$$0 < \int d^3\vec{r}\,\left(V_{\rm ext}(\vec{r}) - V'_{\rm ext}(\vec{r})\right)\left(n'_0(\vec{r}) - n_0(\vec{r})\right). \tag{60}$$

This strict inequality is incompatible with the possibility that $n_0(\vec{r}) = n'_0(\vec{r})$ almost everywhere.

In summary, in this second step we have proved that:

$$|\Psi_0^{(e)}\rangle \neq |\Psi_0^{(e)'}\rangle \rightarrow n_0(\vec{r}) \neq n'_0(\vec{r})\,, \tag{61}$$

which completes the prove that the mapping is injective.

In conclusion, even though there are infinitely many many-body wavefunctions that provide the same density $n(\vec{r})$, the *ground-state many-body wavefunction $|\Psi_0^{(e)}\rangle$ is uniquely determined by the ground-state density $n_0(\vec{r})$*. This is an amazing result, since the amount of information contained in the many-body wavefunction is immensely larger [by an amount proportional to $\exp(N_e)$] than the amount of information contained in a simple function of a 3D vector such as $n_0(\vec{r})$.

Taking the first step into account, we conclude that also the external potential $V_{\rm ext}(\vec{r})$ is uniquely determined by the ground-state density $n_0(\vec{r})$. This second conclusion is far less extraordinary, because $n_0(\vec{r})$ are $V_{\rm ext}(\vec{r})$ both functions of a 3D vector, thus of course one expects a one-to-one correspondence between them.

In other words, this First Theorem allows us to invert the functional dependence outlined in (48), so that

$$n_0(\vec{r}) \rightarrow |\Psi_0^{(e)}[n_0]\rangle \rightarrow V_{\rm ext}[n_0](\vec{r})\,. \tag{62}$$

Given a ground-state density $n_0(\vec{r})$, one can legitimately be sure that a unique ground state many-body wave function and a unique (up to a constant) external potential exist, such that the solution of the many-body Schrödinger problems for the N_e electrons in that external potential provides precisely that given ground-state density.

Of course this existence theorem does not provide any hint how to compute this dependence explicitly.

2.4.1.2. *The Second Theorem.* Let us now prove that even the ground-state energy can be expressed as a functional of the ground-state density alone. Fixed an external potential $V_{\rm ext}(\vec{r})$, the following functional:

$$E_{\rm HK}[n] \equiv \langle\Psi_0^{(e)}[n]|\hat{H}_e^{(R)}|\Psi_0^{(e)}[n]\rangle = \langle\Psi_0^{(e)}[n]|\hat{T}_e + \hat{V}_{ee} + \hat{V}_{\rm ext}|\Psi_0^{(e)}[n]\rangle \tag{63}$$

can be rigourosly defined (for any reasonably well behaved $n(\vec{r})$ in the light of the first theorem. Notice that $|\Psi_0^{(e)}[n]\rangle$ is the (exact) ground state of the Hamiltonian:

$$\hat{T}_e + \hat{V}_{ee} + \hat{V}_{\rm ext}[n]\,, \tag{64}$$

the existence of which is guaranteed by the first theorem. Clearly, if $n = n_0$, $E_{\rm HK}[n_0]$ is the exact ground state energy of our problem defined by the given external potential $V_{\rm ext}(\vec{r})$. Instead, for $n \neq n_0$, $\hat{V}_{\rm ext}[n] \neq \hat{V}_{\rm ext}$, and $|\Psi_0^{(e)}[n]\rangle$ is *not* the ground state of the Hamiltonian $\hat{T}_e + \hat{V}_{ee} + \hat{V}_{\rm ext}$! Therefore $|\Psi_0^{(e)}[n]\rangle$ can be seen as a linear combination involving not just the ground state, but also components of excited states of $\hat{T}_e + \hat{V}_{ee} + \hat{V}_{\rm ext}$, so that

$$E_{\rm HK}[n] > E_{\rm HK}[n_0] \qquad \text{for } n \neq n_0\,. \tag{65}$$

Clearly, if n is precisely the ground-state density n_0, one has $\hat{V}_{\rm ext}[n_0] = \hat{V}_{\rm ext}$ and $E_{\rm HK}[n_0]$ attains its minimum value E_0, smaller than all possible energies $E_{\rm HK}[n]$ obtained with "wrong" densities n.

This observation allows us to write the ground-state energy:

$$E_0 = \min_n E_{\rm HK}[n]\,, \tag{66}$$

subjected to the conservation of particle number: $\int d^3\vec{r}\, n(\vec{r}) = N_e$.

The Hohenberg-Kohn energy functional can be made more explicit:

$$\begin{aligned} E_{\rm HK}[n] &= \langle \Psi_0^{(e)}[n]|\hat{T}_e|\Psi_0^{(e)}[n]\rangle + \langle \Psi_0^{(e)}[n]|\hat{V}_{ee}|\Psi_0^{(e)}[n]\rangle + \langle \Psi_0^{(e)}[n]|\hat{V}_{\rm ext}|\Psi_0^{(e)}[n]\rangle \\ &= \int d^3\vec{r}\, n(\vec{r})\, V_{\rm ext}(\vec{r}) + \frac{e^2}{2}\int d^3\vec{r}\int d^3\vec{r}'\,\frac{n(\vec{r})n(\vec{r}')}{|\vec{r}-\vec{r}'|} + F_{\rm HK}[n]\,. \end{aligned} \tag{67}$$

We express $E_{\rm HK}[n]$ as the sum of the exact term describing the interaction with the external potential, a Hartree energy accounting approximately for the interparticle Coulomb repulsion at a mean-field level, plus a remaining term taking into account the kinetic, exchange, and correlation contributions to the ground-state energy. In practice, Eq. (67) is the *definition* of $F_{\rm HK}[n]$. Its usefulness comes in shifting the difficulty of $E_{\rm HK}[n]$ to a presumbly smaller $F_{\rm HK}[n]$.

2.4.2. An example: the Thomas-Fermi approximation. Numerous approximations of $F_{\rm HK}[n]$ have been proposed. The simplest and oldest of them is the *Thomas-Fermi approximation* (1927). It moves from the observation that, in a uniform and non-interacting Fermi gas the average kinetic energy per electron is $\langle \hat{T}_e\rangle / N_e = {}^3\!/_5\,\hbar^2 k_F^2/(2m_e)$, so that the total kinetic energy per unit volume is:

$$\frac{\langle \hat{T}_e\rangle}{V} = \frac{3}{5}\frac{\hbar^2 k_F^2}{2m_e}\, n \qquad \text{with } k_F(n) = \left(3\pi^2 n\right)^{1/3}. \tag{68}$$

The TF method consists in (i) assuming that this relation holds locally also in a non-homogeneous interacting system, introducing a density of kinetic energy

$$\varepsilon_{\text{kin TF}}(\vec{r}) = \frac{T_{e\,\rm TF}(\vec{r})}{V} = \frac{3}{5}\frac{\hbar^2 k_F^2(n(\vec{r}))}{2m_e}\, n(\vec{r}) \tag{69}$$

and in (ii) neglecting the contributions related to both exchange and correlation effects in $F_{\rm HK}[n]$. We introduce the shorthand $C = \frac{3}{5}\,(3\pi^2)^{2/3}\,\hbar^2/(2m_e)$ and define

$$E_{\text{kin TF}}[n] = \int d^3\vec{r}\,\varepsilon_{\text{kin TF}}(\vec{r}) = C\int d^3\vec{r}\, n(\vec{r})^{5/3}. \tag{70}$$

The TF functional approximates the HK functional as follows:

$$E_{\rm HK}[n] \to E_{\rm TF}[n] = C\int d^3\vec{r}\, n(\vec{r})^{\frac{5}{3}} + \frac{e^2}{2}\int d^3\vec{r}\int d^3\vec{r}'\,\frac{n(\vec{r})n(\vec{r}')}{|\vec{r}-\vec{r}'|} + \int d^3\vec{r}\, n(\vec{r})\, V_{\rm ext}(\vec{r})\,. \tag{71}$$

The equation for the ground-state density is obtained by equating to zero the functional derivative of $E_{\rm TF}[n]$ with respect to the density itself:

$$\frac{\delta}{\delta n(\vec{r})}\left(E_{\rm TF}[n] - \mu\left[\int d^3\vec{r}\, n(\vec{r}) - N_e\right]\right) = 0\,, \tag{72}$$

where the second term is a Lagrange multiplier needed to fix the density normalization to the number of particles N_e. Of course, μ is a constant, independent of $\vec{r}$, and represents the chemical potential of the electrons.

By evaluating the functional derivative, the resulting *Thomas-Fermi equation* is:

$$\frac{5}{3}Cn(\vec{r})^{\frac{2}{3}} + e^2\int d^3\vec{r}'\,\frac{n(\vec{r}')}{|\vec{r}-\vec{r}'|} + V_{\rm ext}(\vec{r}) = \mu\,. \tag{73}$$

This is an integral functional equation for n, which, for given $V_{\rm ext}(\vec{r})$ and μ, is usually solved iteratively.

The TF functional can be improved by the addition of an exchange term [**6**]. The exchange energy per electron of the homogeneous electron gas only depends on the density, and can be calculated exactly:

$$\frac{E_{\rm x}(n)}{N_e} = -\frac{3}{4}\left(\frac{3}{\pi}\right)^{1/3} e^2\, n^{1/3}\,. \tag{74}$$

In the same spirit as for the kinetic term, this suggests adding

$$E_{\rm x}[n] = C' \int d^3\vec{r}\, n(\vec{r})^{\frac{4}{3}} \tag{75}$$

to the TF energy for the nonhomogeneous situation. Here the constant $C' = -\frac{3}{4}\,(3/\pi)^{1/3}\, e^2$. This addition to the functional introduces an extra exchange term at the left side of the TF equation (73), namely:

$$\frac{4}{3}C' n(\vec{r})^{1/3}. \tag{76}$$

The self-consistent solution can be sought by rearranging the TF equation as follows:

$$\begin{aligned}
\frac{5}{3}Cn(\vec{r})^{\frac{2}{3}} =& \mu - e^2 \int d^3\vec{r}'\, \frac{n(\vec{r}')}{|\vec{r}-\vec{r}'|} - V_{\rm ext}(\vec{r}) - \frac{4}{3}C' n(\vec{r})^{1/3} \\
n(\vec{r})^{\frac{2}{3}} =& \frac{3}{5C}\left[\mu - e^2 \int d^3\vec{r}'\, \frac{n(\vec{r}')}{|\vec{r}-\vec{r}'|} - V_{\rm ext}(\vec{r}) - \frac{4}{3}C' n(\vec{r})^{1/3}\right] \\
n(\vec{r}) =& \begin{cases} \left(\frac{3}{5C}\left[\mu - e^2 \int d^3\vec{r}'\, \frac{n(\vec{r}')}{|\vec{r}-\vec{r}'|} - V_{\rm ext}(\vec{r}) - \frac{4}{3}C' n(\vec{r})^{1/3}\right]\right)^{3/2} & \text{usually} \\ 0 \qquad \text{at locations } \vec{r} \text{ where the argument of } (\cdot)^{3/2} \text{ is negative} \end{cases}
\end{aligned} \tag{77}$$

One starts from an arbitary $n(\vec{r})$, plugs it in the right hand side of Eq. (77), obtains a new $n(\vec{r})$, and iterates this substitution until convergence is achieved. Clearly, for an arbitrarily picked μ, at the end of the self-consistent solution of Eq. (73), one usually obtains an incorrect number of electrons $\int d^3\vec{r}\, n(\vec{r}) \neq N_e$. One can then repeat the calculation, adjusting μ until the correct normalization of the density is obtained.

For examples of the implementation of Eq. (73) in atomic and molecular physics, see e.g. Ref. [**7, 8**].

The TF approximation is numerically quite cheap, but, alas, its accuracy is very very poor in the description of situations where the electron density changes significantly over scales of the order of a_0. Unfortunately this is always the case in condensed matter. As an example of unphysical behavior of the solutions of Eq. (77), note that the density vanishes in the "classically forbidden" regions where $\mu - V_{\rm ext}(\vec{r}) < 0$. This feature implies the lack of all kinds of evanescent waves, long-distance decay of the density, and the associated quantum tunneling effects. An even worst drawback of the TF approximation, is that of predicting no bonding! For any two atoms, the adiabatic potential computed in the TF approximation is a monotonically decreasing function of the interatomic distance [**8**]: it shows no minimum, thus no molecular bond.

2.4.3. The Kohn-Sham method. The Second Theorem guarantees that there exists an exact Hohenberg-Kohn energy functional. We need to determine a practical much better approximation than the one provided by the TF model. To this purpose, consider a system of N_e interacting electrons in some external potential $V_{\rm ext}(\vec{r})$, and denote its exact ground-state density with $n_0(\vec{r})$.

The HK theorem is not specific of the Coulomb e-e interaction: it is a general many-body theorem that applies to identical particles interacting with any arbitrary 2-body interparticle interaction. Of course, the corresponding HK functional will be different depending on the choice of the modified $\hat{V}_{ee}$. Consider for example the special and interesting case $\hat{V}_{ee} = 0$, i.e. *non-interacting* electrons. Given a density $n_0(\vec{r})$ (here we focus on the exact density of the true interacting electrons, but any density here

would do), by virtue of the First HK theorem, there exists a unique fictitious external potential $\tilde{V}_{\rm ext}[n]$ such that a system of N_e non-interacting electrons subjected to $\tilde{V}_{\rm ext}[n_0]$ has ground-state density n_0.

The system of non-interacting particles has the advantage that we do know its ground-state wave function. It is a Slater determinant:

$$\Psi^{(e)}_{\rm KS}(w_1 \dots w_{N_e}) = \frac{1}{\sqrt{N_e!}} \begin{vmatrix} \phi_1(w_1) & \dots & \phi_{N_e}(w_1) \\ \dots & \dots & \dots \\ \phi_1(w_{N_e}) & \dots & \phi_{N_e}(w_{N_e}) \end{vmatrix} \tag{78}$$

of single-particle orbitals $\phi_k(w)$ called *Kohn-Sham wavefunctions* that solve the single-electron Schrödinger equation associated to $\tilde{V}_{\rm ext}[n_0]$. Note that, even though we use the same symbol, these single-particle states $|\phi_k\rangle$ are generally different from the HF ones. For this state $|\Psi^{(e)}_{\rm KS}\rangle$, the density and the kinetic energy take the forms:

$$n(\vec{r}) = \sum_{i=1}^{N_e} \sum_{\sigma} |\phi_i(\vec{r},\sigma)|^2, \tag{79}$$

$$E_{\rm kin\,KS} = -\frac{\hbar^2}{2m} \sum_{i=1}^{N_e} \sum_{\sigma} \int d^3\vec{r}\, \phi_i(\vec{r},\sigma)^* \Delta_{\vec{r}}\, \phi_i(\vec{r},\sigma) = \frac{\hbar^2}{2m} \sum_{i=1}^{N_e} \sum_{\sigma} \int d^3\vec{r}\, |\nabla_{\vec{r}}\, \phi_i(\vec{r},\sigma)|^2. \tag{80}$$

Notice that the expression of $n(\vec{r})$ in terms of single-particle orbitals is exact, and that we insist that the ground state of the interacting system and that of the fictitious non-interacting system share the same density n_0. However, the wavefunction is obviously different $|\Psi^{(e)}_0\rangle \neq |\Psi^{(e)}_{\rm KS}\rangle$, which implies that the expression (80) for the kinetic energy is only approximate. In practice, the $E_{\rm kin\,KS}$ of Eq. (80) does not take into account the additional contributions to the true kinetic energy induced by the presence of electron-electron correlations. Despite these warnings, $E_{\rm kin\,KS}$ is far better approximation to the true $E_{\rm kin}$ than $E_{\rm kin\,TF}$, Eq. (70).

To take advantage of this better estimation of the kinetic energy, we introduce it explicitly in the Kohn-Sham formulation of the Hohenberg-Kohn energy functional:

$$E_{\rm HK}[n] = E_{\rm kin\,KS} + \int d^3\vec{r}\, n(\vec{r})\, V_{\rm ext}(\vec{r}) + \frac{e^2}{2} \int d^3\vec{r} \int d^3\vec{r}\,' \frac{n(\vec{r}) n(\vec{r}\,')}{|\vec{r} - \vec{r}\,'|} + E_{\rm xc}[n]\,. \tag{81}$$

Here the exchange-correlation contribution $E_{\rm xc}[n]$ takes into account all Coulomb exchange and correlation effects (i.e. the difference between the exact $\langle \Psi^{(e)}_0[n]|\hat{V}_{ee}|\Psi^{(e)}_0[n]\rangle$ and the Hartree energy $E_{\rm Hartree}[n]$), as well as the difference between the exact and the Kohn-Sham (non-interacting electrons) kinetic energy. In practice Eq. (81) is the definition of $E_{\rm xc}[n]$. The advantage of the KS formulation (81) over the original HK formulation (67) is that the less well characterized term $E_{\rm xc}[n]$ is usually far smaller than $F_{\rm HK}[n]$.

The ground-state energy is the minimum value of the energy functional, the minimum being taken with respect to all Kohn-Sham single-particle orbitals and under the constraint that the KS orbitals be orthonormal, i.e.:

$$\int dw\, \phi^*_i(w)\, \phi_j(w) = \delta_{ij}\,, \tag{82}$$

the same as for the HF equation. The equation defining the Kohn-Sham orbitals is found by minimizing the GS-energy functional under the constraint of Eq. (82), with the (by now standard) technique of the matrix λ_{ij} of Lagrange multipliers, that we assume to be diagonal, with eigenvalues ϵ_k.

To write the KS equation, we take the functional derivative of $E_{\rm HK}[n]$, Eq. (81), with respect to the Kohn-Sham orbitals. We introduce $V_{\rm Hartree}[\vec{r},n]$:

$$\frac{\delta}{\delta\phi_k^*(w)}E_{\rm Hartree}[n] = \int d^3\vec{r}'\frac{e^2}{|\vec{r}-\vec{r}'|}n(\vec{r}')\,\phi_k(w) \equiv V_{\rm Hartree}[\vec{r},n]\,\phi_k(w) \tag{83}$$

with $w=(\vec{r},\sigma)$, see Eq. (43). Likewise,

$$\frac{\delta}{\delta\phi_k^*(w)}E_{\rm xc}[n] = \frac{\delta E_{\rm xc}[n]}{\delta n(\vec{r})}\,\phi_k(w) = V_{\rm xc}[\vec{r},n]\,\phi_k(w) \tag{84}$$

defines the exchange and correlation potential $V_{\rm xc}[\vec{r},n]$.

In terms of these quantities, the *Kohn-Sham equation* is

$$\left(-\frac{\hbar^2}{2m_e}\Delta_{\vec{r}} + V_{\rm ext}(\vec{r}) + V_{\rm Hartree}[\vec{r},n] + V_{\rm xc}[\vec{r},n]\right)\phi_k(w) = \epsilon_k\,\phi_k(w)\,. \tag{85}$$

In practice this equation defines the effective potential acting on the noninteracting electrons

$$\tilde{V}_{\rm ext}[n_0] = V_{\rm ext}(\vec{r}) + V_{\rm Hartree}[\vec{r},n_0] + V_{\rm xc}[\vec{r},n_0]\,, \tag{86}$$

and giving the same density as the real interacting system, as introduced above.

The Kohn-Sham equation (85) is structurally similar to the Hartree-Fock equation (47). They are both nonlinear equations for independent-electron wavefunctions, which can be seen as linear Schrödinger-like equations, but with a potential that depends on the eigenfunctions themselves, requiring a self-consistent solution.

The technical novelty of the KS equation is that the *exchange-correlation potential is local*, a simple multiplicative operator, unlike the Fock exchange potential of the HF equation. This difference makes the KS method highly advantageous compared to the HF method, because nonlocal terms are usually far more costly computationally.

The KS equation provides a practical scheme for introducing the description of correlations beyond what is done in the Hartree-Fock method, which only includes correlations arising from the Pauli exclusion principle, through the exchange term.

On the other hand, the parameterization of the electron density in terms of the KS single-electron orbitals constitutes a sort of betrayal of the original spirit of the DFT, which brings the KS method at a level of computational cost and technical involvedness comparable to that of HF. In particular the need to store N_e single-electron orbitals rather than just one density function n limits the applicability of this method to the simulation of relatively few electrons, say $10^2 \div 10^3$. The simulation of solids, that involve macroscopic numbers of electrons, requires special tricks that we shall describe later on in the course.

Once the Kohn-Sham equation are solved iteratively, the ground-state energy can be computed by inserting the self-consistent (KS) wavefunctions into the expression of the energy functional (81). An alternative expression for the total electronic energy is

$$E_{\rm KS}[n] = \sum_{k=1}^{N_e}\epsilon_k - E_{\rm Hartree}[n] + E_{\rm xc}[n] - \int d^3\vec{r}\,V_{\rm xc}[\vec{r},n]\,n(\vec{r})\,. \tag{87}$$

Notice that the last three terms are needed to correct for differences between the expressions of the nonlinear terms in the expressions for the total energy $E_{\rm HK}[n]$ and for the average value of the effective potential (86). The latter enters the KS eigenvalues ϵ_k, and must then be corrected for.

To use the KS method concretely, some reliable approximation of the exchange-correlation functional must be adopted. Notice that in a few very special cases, the exchange-correlation potential can

be written exactly. For example, in the limiting case in which the system consists of a single electron subjected to some external potential $V_{\rm ext}$, the Schrödinger equation reduces to

$$\left(-\frac{\hbar^2}{2m}\Delta + V_{\rm ext}(\vec{r})\right)\phi(\vec{r}) = \varepsilon\phi(\vec{r})\,. \tag{88}$$

The Kohn-Sham equation are immediately recovered if we identify $\phi(\vec{r})$ with the (only) KS wavefunction, $\varepsilon = E_0$, and $V_{\rm xc}[\vec{r}, n] = -V_{\rm Hartree}[\vec{r}, n] = -\int d^3\vec{r}' n(\vec{r}')\, e^2/|\vec{r} - \vec{r}'|$.

2.4.3.1. *The local-density approximation (LDA).* For more interesting many-electrons systems, the simplest approximation to $E_{\rm xc}[n]$ is the *local-density approximation* (LDA), in which the exchange-correlation contribution is expressed as the integral over the entire space of a function of the density at each point:

$$E_{\rm xc}^{\rm LDA}[n] = \int d^3\vec{r}\, \varepsilon_{\rm xc}^{\rm HEG}(n(\vec{r}))\, n(\vec{r})\,, \tag{89}$$

where $\varepsilon_{\rm xc}^{\rm HEG}(n)$ is the exchange-correlation energy per electron of a homogeneous electron gas (HEG) of density n. This expression follows the spirit of the Thomas-Fermi method, except that this local approximation is applied to the exchange and correlation energy, a usually far smaller energy contribution than the kinetic energy which is approximated locally by the TF method.

$\varepsilon_{\rm xc}^{\rm HEG}(n)$ is a real function of a single variable, which makes it conceptually simple to evaluate and store. In the limiting cases of low and high density, $\varepsilon_{\rm xc}^{\rm HEG}(n)$ can be evaluated analytically by means of many-body perturbation theory. Data from quantum Monte Carlo simulations can provide $\varepsilon_{\rm xc}^{\rm HEG}(n)$ for arbitrary intermediate densities. Standard DFT computer codes implement interpolated formulas for $\varepsilon_{\rm xc}^{\rm HEG}(n)$, matching the asymptotic expressions and QMC data. Taking the functional derivative of $E_{\rm xc}^{\rm LDA}[n]$, $V_{\rm xc}^{\rm LDA}$ is then given by

$$V_{\rm xc}^{\rm LDA}(n(\vec{r})) = n(\vec{r})\left.\frac{d\varepsilon_{\rm xc}^{\rm HEG}(n)}{dn}\right|_{n=n(\vec{r})} + \varepsilon_{\rm xc}^{\rm HEG}(n(\vec{r}))\,.$$

Here the derivative is a plain function derivative, not a functional one. The first QMC simulation studies of the HEG date back to the 1970's and 1980's [**9**]. In 1980 Perdew and Zunger proposed a first viable analytical interpolation of the QMC data available at that time [**10**]. Further refinements of the $\varepsilon_{\rm xc}^{\rm HEG}(n)$ function have been published in the following decades.

By construction, the local LDA is exact for the HEG. In practical conditions where the density changes with position, the LDA is known to work fairly well and provide reasonably accurate energetics. One of the hardest problems for DFT-LDA is that of 1 electron in a strongly nonhomogeneous condition. The H atom in LDA has a total energy of −12.1 eV, compared to the exact (and HF) value −13.6 eV. In more standard many-electron conditions, errors are percentually smaller. In system composed by many atoms, LDA usually tends to overbind (by a few percent).

Improvements over the LDA have been introduced, e.g. with functionals depending on the gradient of the density (GGA).

2.5. Comparison of HF and DFT

HF starts from an approximation to the wavefunction. DFT is in principle exact.

The fundamental variable of DFT is the density n, not the wavefunction as in HF.

For the GS, HF is variational, $E_{\rm HF} \geq E_0$.

DFT is in principle exact $E_{\rm DFT} = E_0$, but approximate DFT (e.g. LDA) is non variational $E_{\text{DFT-LDA}} <=> E_0$.

HF can be applied to the GS or to an excited state. DFT in an intrinsically GS theory (but extensions such as time-dependent DFT are available).

The dependence of the total energy on the position of the nuclei R (through $V_{\rm ext}$) can be minimized to obtain the equilibrium structure. Both DFT and HF usually provide equilibrium structures close to experiment.

The HF Fock exchange term is nonlocal. The DFT $V_{\rm xc}[\vec{r}, n]$ potential is local.

When we come to electrons and electronic states, we will discuss the significance of the HF and KS single-electron eigenvalues ϵ_k. A little anticipation: HF tends to overestimate the energy gap between occupied and empty states. DFT tends to underestimate it.

In practice, for extended systems (e.g. solids) DFT is by far the most popular method.

2.6. Crystal vibrations

Phonons are the quanta of the harmonic oscillations around the minimum of $V_{\rm ad}(R)$.

See Kittel [**1**], Chap. 4 and 5, plus Grosso Pastori-Parravicini [**3**], Chap. 9.

2.6.1. Equation of state of a crystal and thermal expansion. For this part we follow Ashcroft's book [**2**], Chap. 25. We recall that

$$P = -\left.\frac{\partial F}{\partial V}\right|_T . \tag{90}$$

Here the free energy

$$F = U - TS = -\frac{\log Z}{\beta} = -k_{\rm B}T \log Z . \tag{91}$$

For an insulating crystal

$$F = U_{\rm minimum} + F_{\rm oscillators}(V,T) . \tag{92}$$

$U_{\rm minimum}$ coincides with the minimum value of $V_{\rm ad}$ at the equilibrium crystal structure and volume. $F_{\rm oscillators}(V,T)$ contains the contribution of the quantum oscillators. In the harmonic approximation:

$$F_{\rm oscillators}(V,T) = \sum_{\vec{k},s} F_{1\,\vec{k},s} = \sum_{\vec{k},s} F_{1\,\omega_{\vec{k},s}} . \tag{93}$$

Each term corresponds to an independent harmonic oscillator. Its partition function

$$Z_{1\,\omega} = \sum_{v=0}^{\infty} e^{-\frac{\hbar\omega}{k_{\rm B}T}(\frac{1}{2}+v)} = e^{-\frac{1}{2}\frac{\hbar\omega}{k_{\rm B}T}} \sum_{v=0}^{\infty} e^{-\frac{\hbar\omega}{k_{\rm B}T}v} = e^{-\frac{1}{2}\frac{\hbar\omega}{k_{\rm B}T}} \sum_{v=0}^{\infty} \left(e^{-\frac{\hbar\omega}{k_{\rm B}T}}\right)^v = e^{-\frac{1}{2}\frac{\hbar\omega}{k_{\rm B}T}} \frac{1}{1-e^{-\frac{\hbar\omega}{k_{\rm B}T}}} . \tag{94}$$

Whence

$$\begin{aligned} F_{1\,\omega} =& -k_{\rm B}T \log\left(e^{-\frac{1}{2}\frac{\hbar\omega}{k_{\rm B}T}} \frac{1}{1-e^{-\frac{\hbar\omega}{k_{\rm B}T}}}\right) = -k_{\rm B}T \left(\log e^{-\frac{1}{2}\frac{\hbar\omega}{k_{\rm B}T}} + \log \frac{1}{1-e^{-\frac{\hbar\omega}{k_{\rm B}T}}}\right) \\ =& k_{\rm B}T \left(\log e^{\frac{1}{2}\frac{\hbar\omega}{k_{\rm B}T}} + \log(1-e^{-\frac{\hbar\omega}{k_{\rm B}T}})\right) = \frac{1}{2}\hbar\omega + k_{\rm B}T \log(1-e^{-\frac{\hbar\omega}{k_{\rm B}T}}) , \end{aligned} \tag{95}$$

see Fig. 2.2.

To compute the pressure we need the ingredient

$$\left.\frac{\partial F_{1\,\omega}}{\partial V}\right|_T = \frac{1}{2}\frac{\partial\hbar\omega}{\partial V} + k_{\rm B}T \frac{e^{-\frac{\hbar\omega}{k_{\rm B}T}}}{1-e^{-\frac{\hbar\omega}{k_{\rm B}T}}} \frac{1}{k_{\rm B}T} \frac{\partial\hbar\omega}{\partial V} = \left(\frac{1}{2} + \frac{1}{e^{\frac{\hbar\omega}{k_{\rm B}T}}-1}\right)\frac{\partial\hbar\omega}{\partial V} . \tag{96}$$

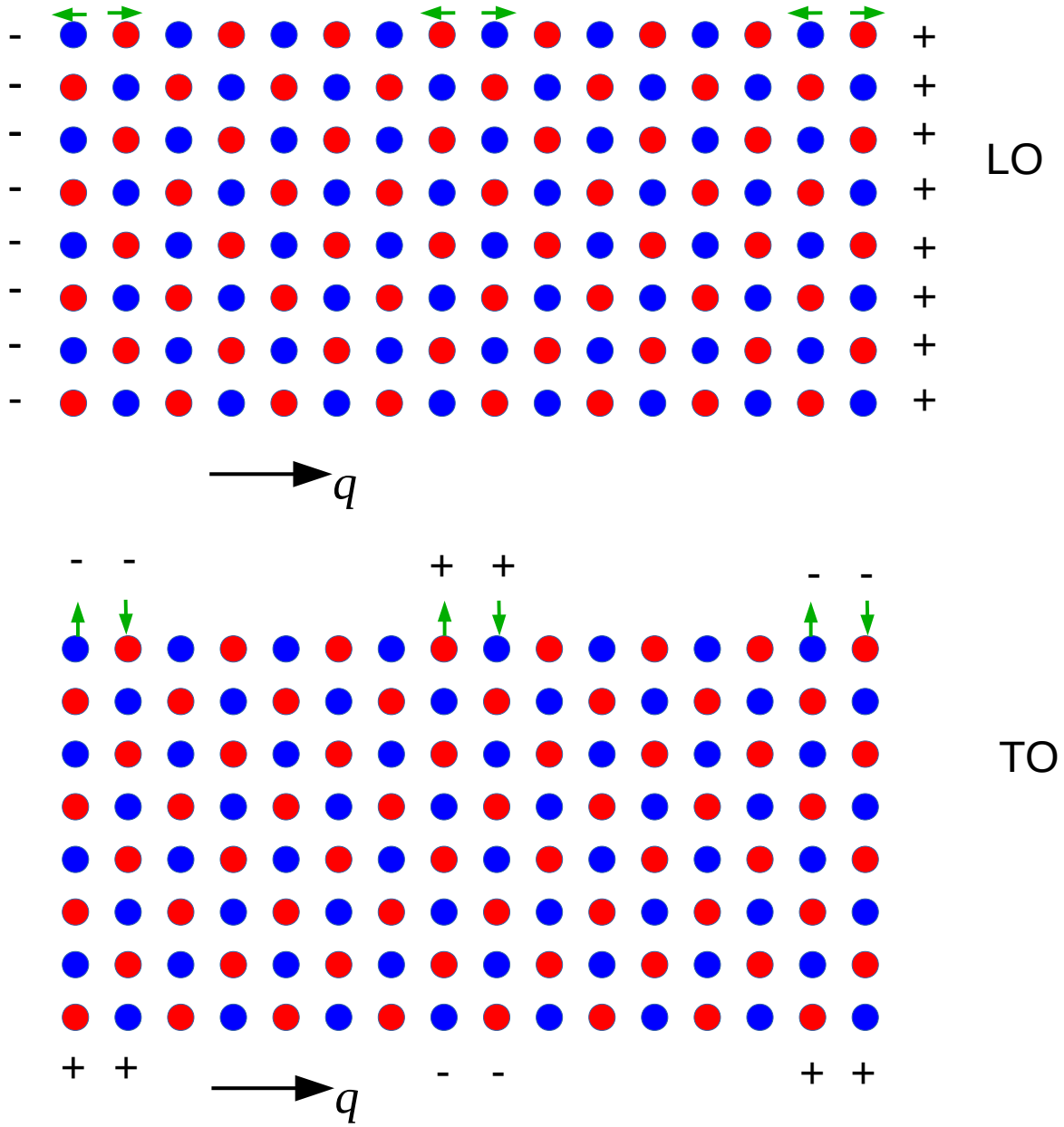

FIGURE 2.1. A sketch of instant displacements for the optical phonons of a cubic ionic crystal, explaining the reason for different LO and TO frequencies at small (nonzero) wavevector q.

With this result we reconstruct the pressure:

$$P = -\frac{\partial V_{\text{ad}}(\text{equilibrium}, V)}{\partial V} + \sum_{\vec{k},s} \left[\frac{1}{2} + \underbrace{\frac{1}{\exp\left(\frac{\hbar\omega_{\vec{k},s}}{k_{\text{B}}T}\right) - 1}}_{[v_{\vec{k},s}]}\right] \left(-\frac{\partial \hbar\omega_{\vec{k},s}}{\partial V}\right). \tag{97}$$

For exactly harmonic oscillators, we foresee *no thermal expansion*, because the $\hbar\omega_{\vec{k},s}$ do not depend on volume, see Fig. 2.3: in a harmonic crystal, pressure does not change as a function of temperature.

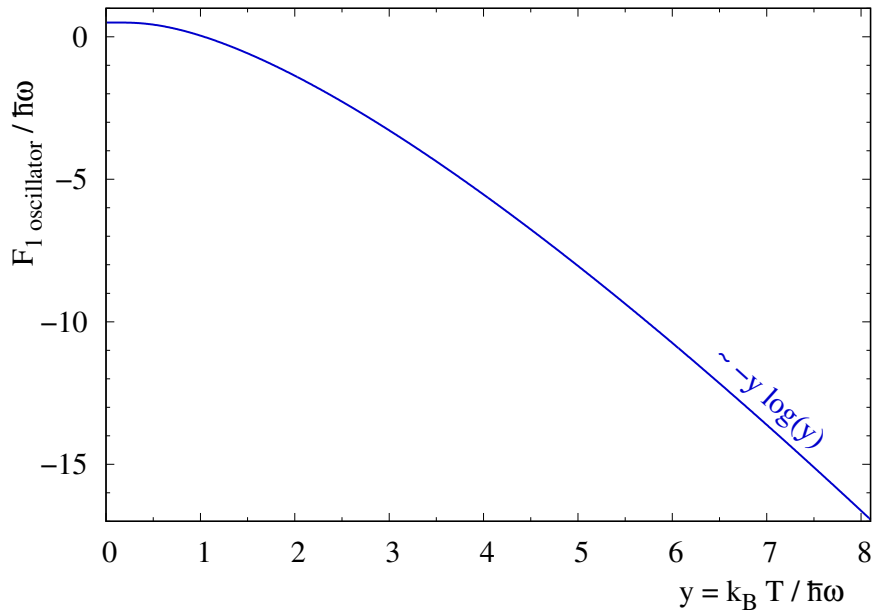

FIGURE 2.2. The temperature dependence of the free energy of a quantum harmonic oscillator.

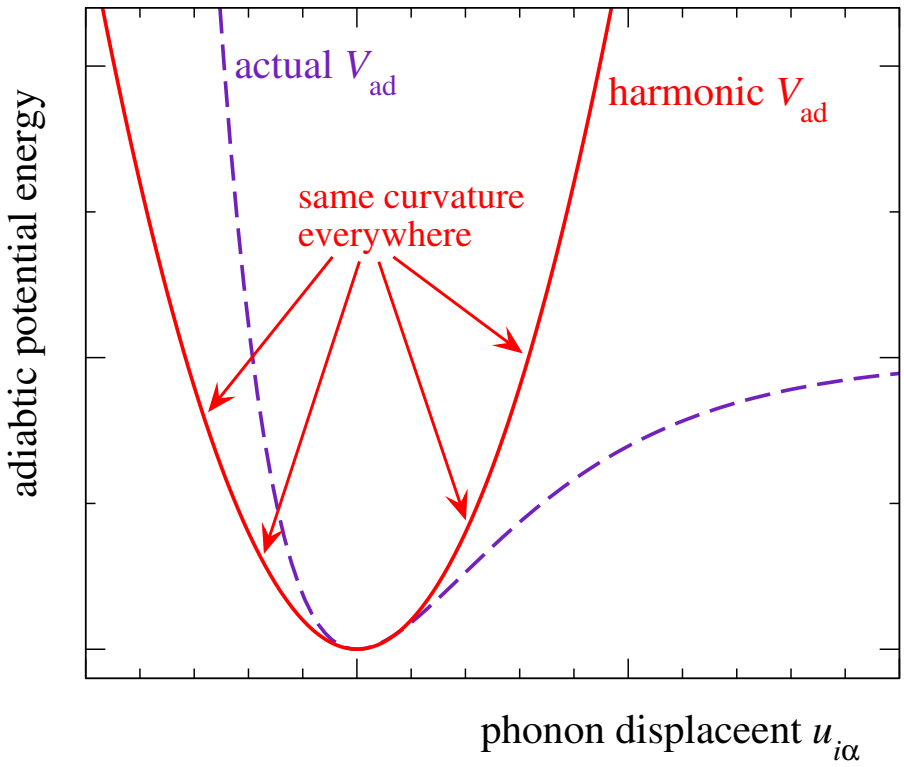

FIGURE 2.3. A sketch of a cut of adiabatic potential along one of the phonon normal coordinates: comparison of the actual potential with the harmonic approximation.

To study the thermal expansion we need to assume therefore that the frequencies are affected by volume, as occurs in real-life *anharmonic* solids. We target the standard experimental conditions,

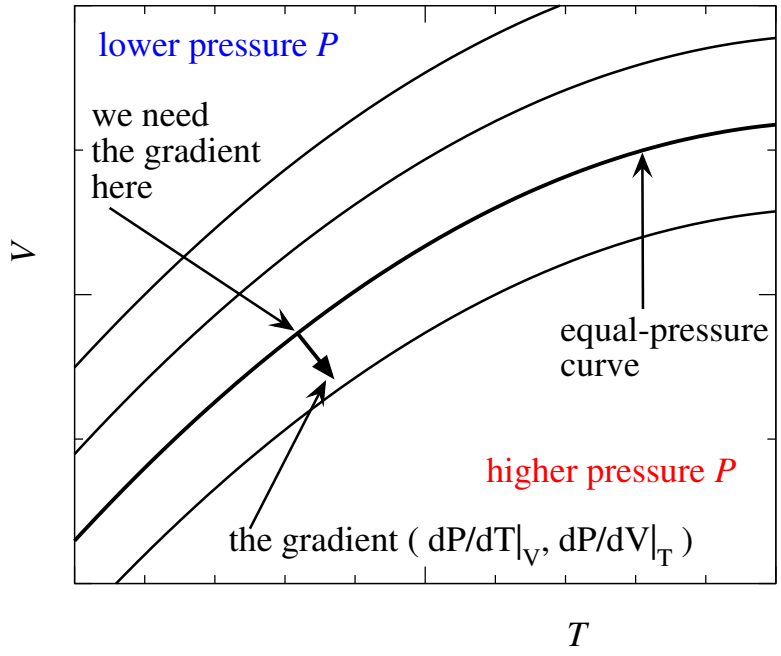

FIGURE 2.4. An illustration of the relation (98). $\left(\frac{\partial V}{\partial T}\right)_P$ is precisely the slope of a isobaric curve in this $T-V$ phase diagram. To obtain this slope, we observe that it is perpendicular to the gradient of pressure as a function of these two variables T and V. This gradient is a vector with components $\left(\left(\frac{\partial P}{\partial T}\right)_V, \left(\frac{\partial P}{\partial V}\right)_T\right)$. To obtain the needed slope, we need to apply a 90° rotation, which generates the rotated vector $\left(\left(\frac{\partial P}{\partial V}\right)_T, -\left(\frac{\partial P}{\partial T}\right)_V\right)$. The needed slope of the isobaric curve is the ratio of the y to the x component of this vector, namely Eq. (98).

namely fixed pressure P:

$$\left(\frac{\partial V}{\partial T}\right)_P = -\frac{\left(\frac{\partial P}{\partial T}\right)_V}{\left(\frac{\partial P}{\partial V}\right)_T} . \tag{98}$$

For a justification for this formula, see Fig. 2.4.

The coefficient of linear expansion:

$$\alpha = \frac{1}{\ell}\left(\frac{\partial \ell}{\partial T}\right)_P = \frac{1}{3V}\left(\frac{\partial V}{\partial T}\right)_P = -\frac{1}{3V}\frac{\left(\frac{\partial P}{\partial T}\right)_V}{\left(\frac{\partial P}{\partial V}\right)_T} = \frac{1}{3}\left(\frac{\partial P}{\partial T}\right)_V \frac{1}{-V\left(\frac{\partial P}{\partial V}\right)_T} = \frac{1}{3B}\left(\frac{\partial P}{\partial T}\right)_V . \tag{99}$$

Therefore, substituting the espression (97):

$$\alpha = \frac{1}{3B}\sum_{\vec{k},s}\left(-\frac{\partial \hbar\omega_{\vec{k},s}}{\partial V}\right)\frac{\partial [v_{\vec{k},s}]}{\partial T} . \tag{100}$$

Compare this expression with that of heat capacity at fixed volume and per unit volume:

$$c_V = \frac{1}{V}\sum_{\vec{k},s}\hbar\omega_{\vec{k},s}\frac{\partial [v_{\vec{k},s}]}{\partial T} , \tag{101}$$

obtained from $U_{1\vec{k},s} = \hbar\omega_{\vec{k},s}\left([v_{\vec{k},s}] + 1/2\right)$.

This comparison makes it natural to define:

$$c_{V\vec{k},s} = \frac{1}{V}\hbar\omega_{\vec{k},s}\frac{\partial[v_{\vec{k},s}]}{\partial T}\,, \tag{102}$$

the contribution of mode $\vec{k}, s$ to the total heat capacity per unit volume.

Comparing Eqs. (100) and (101), we define also

$$\gamma_{\vec{k},s} = -\frac{V}{\omega_{\vec{k},s}}\frac{\partial\omega_{\vec{k},s}}{\partial V}\,, \tag{103}$$

called the *Grüneisen parameter* for mode $\vec{k}, s$.

We then define the overall Grüneisen parameter for the crystal as

$$\gamma = \frac{\sum_{\vec{k},s}\gamma_{\vec{k},s}c_{V\vec{k},s}}{\sum_{\vec{k},s}c_{V\vec{k},s}}\,, \tag{104}$$

namely a weighted average, the weights being the contributions of the individual modes to the total heat capacity.

With this definition, comparing (100) with (104), we conclude that

$$\alpha = \frac{\gamma c_V}{3B}\,. \tag{105}$$

Since the dimensions of c_V are energy×temperature^{-1}×volume^{-1} and those of the bulk modulus are energy×volume^{-1}, α is correctly an inverse temperature. The typical magnitude of alpha for standard rigid crystals is $\alpha \sim 10^{-5}$ K^{-1}.

Equation (104) tells us that in case all $\gamma_{\vec{k},s}$ happen to be the same, independent of $\vec{k}, s$, then the weighted average is has no effect, and

$$\gamma = \gamma_{\vec{k},s} = -\frac{V}{\omega_{\vec{k},s}}\frac{\partial\omega_{\vec{k},s}}{\partial V} = -\frac{\partial\log\omega_{\vec{k},s}}{\partial\log V}\,. \tag{106}$$

For example in a "Debye crystal", all frequencies scale as $\omega_{\rm D}$, and therefore

$$\gamma = -\frac{\partial\log\omega_{\rm D}}{\partial\log V}\,. \tag{107}$$

Recall that

$$\omega_{\rm D} = v_{\rm s}\left(6\pi^2\frac{N}{V}\right)^{1/3} \propto V^0\,. \tag{108}$$

because $v_{\rm s} \propto a\sqrt{C/M}$ and $a \propto V^{1/3}$ for a harmonic crystal where the coupling strength C does not depend on volume. If however the crystal has some anharmonicity, so that C does depend on volume, one can assume that $\omega_{\rm D} \propto V^{-\eta}$. In this condition, $\log\omega_{\rm D} = -\eta\log V + \text{constant}$, so that $\gamma = \eta$.

LINEAR EXPANSION COEFFICIENTS AND GRÜNEISEN PARAMETERS FOR SOME ALKALI HALIDES

T (K)		LiF	NaCl	NaI	KCl	KBr	KI	RbI	CsBr
0	α	0	0	0	0	0	0	0	0
	γ	1.70	0.90	1.04	0.32	0.29	0.28	−0.18	2.0
20	α	0.063	0.62	5.1	0.74	2.23	4.5	6.0	10.0
	γ	1.60	0.96	1.22	0.53	0.74	0.79	0.85	—
65	α	3.6	15.8	27.3	17.5	22.5	26.0	28.0	35.2
	γ	1.59	1.39	1.64	1.30	1.42	1.35	1.35	—
283	α	32.9	39.5	45.1	36.9	38.5	40.0	39.2	47.1
	γ	1.58	1.57	1.71	1.45	1.49	1.47	—	2.0

[a] The units of the linear expansion coefficient α are in 10^{-6} K^{-1}.
Source: G. K. White, *Proc. Roy Soc. London* **A286**, 204 (1965).

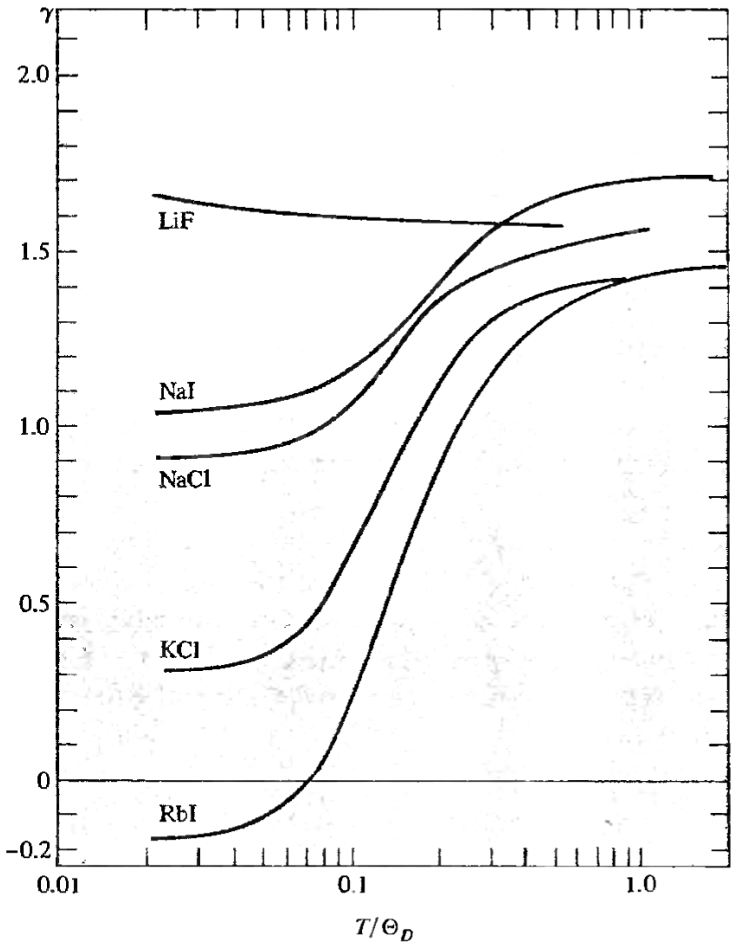

Figure 25.1
Grüneisen parameter vs. T/Θ_D for some alkali halide crystals. (From G. K. White, *Proc. Roy Soc. London* **A286**, 204 (1965).)

B is typically weakly dependent on temperature. In simple systems where all $\gamma_{\vec{k},s}$ happen to be the same, independent of $\vec{k}$, s, also γ is independent of temperature (typically $0.2 \leq \gamma \leq 2$).

In these simple cases one has approximately $\alpha \propto c_V$, which goes as T^3 for small temperature $T \ll \theta_{\mathrm{D}}$ and goes to a constant for large $T \gg \theta_{\mathrm{D}}$.

For real solids γ does change with temperature, see figure in previous page. It may even turn negative, see RbI!

For *metals* we must include the electronic contribution to pressure:

$$P^{\mathrm{el}} = \frac{2}{3}\frac{U^{\mathrm{el}}}{V} \,. \tag{109}$$

$$\left(\frac{\partial P^{\mathrm{el}}}{\partial T}\right)_V = \frac{2}{3V}\left(\frac{\partial U^{\mathrm{el}}}{\partial T}\right)_V = \frac{2}{3}c_V^{\mathrm{el}} \,. \tag{110}$$

Like above, c_V^{el} is per unit volume.

Combining the phononic and the electronic contributions:

$$\alpha = \frac{1}{3B}\left(\gamma c_V^{\mathrm{vibr}} + \frac{2}{3}c_V^{\mathrm{el}}\right) \,. \tag{111}$$

The linear-in-T c_V^{el} is only significant at low temperature $T \lesssim 10$ K. However, this electronic contribution makes $\alpha \propto T$ in metals at low temperature, a qualitative difference compared to insulators.

CHAPTER 3

Electronic structure

3.1. The simplest model for electrons in metals: free electrons

Alias: **the 3D jellium model**, **the 3D homogeneous electron gas**.

Electrons are negatively charged: it is practically impossible to maintain a sizable density of electrons in an extended region of space without some compensating charge.

Constant background charge → vanishing electric field → constant electric potential → plane-wave solution for the electronic wave functions in the (KS) independent-electron picture.
[NB! OK for normal densities, but wrong at low density: spontaneous symmetry breaking → *Wigner crystal*]

Free-electron density of orbital states:

(112) $$\text{in } \vec{k} \text{ space: } g_k = \frac{V}{8\pi^3}$$

Kinetic energy $\hbar^2 k^2/(2m_e)$ increasing with $|\vec{k}|$.

Thus at $T = 0$, states are filled below a max $|\vec{k}| = k_\mathrm{F}$ and empty above. This defines a Fermi sphere, Fig. 3.1.

(113) $$\text{The "volume" of the Fermi sphere} = \frac{4}{3}\pi k_\mathrm{F}^3$$

(114) $$\text{number of states in Fermi sphere, i.e. with } k \le k_\mathrm{F} = g_k \frac{4\pi}{3} k_\mathrm{F}^3 = \frac{V}{6\pi^2} k_\mathrm{F}^3 .$$

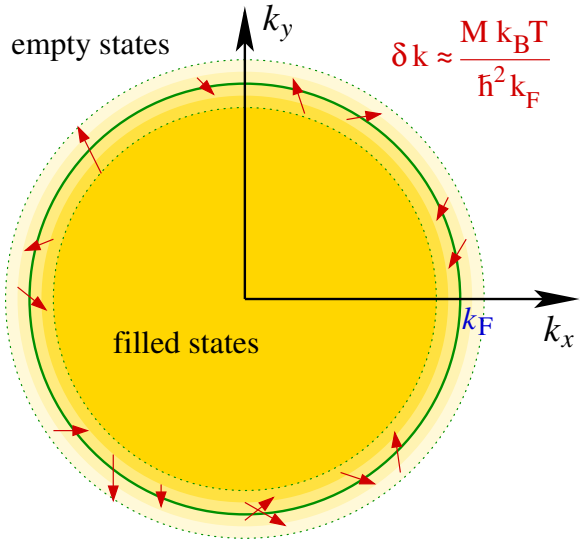

FIGURE 3.1. Thermal excitations/deexcitations across the Fermi sphere involve mainly states within a skin region with thickness $\delta k \propto k_\mathrm{B}T$ across the Fermi sphere. Here this skin thickness is greatly exaggerated, compared to the occupation smearing induced by a realistic temperature $T \ll T_\mathrm{F}$ of electrons in ordinary metals at room conditions

To be multiplied by $g_s = 2$ to account for spin.

The total number of electrons

$$N = \frac{V}{3\pi^2} k_{\rm F}^3 \tag{115}$$

yields the relations between $k_{\rm F}$ and the density $n = N/V$:

$$n = \frac{k_{\rm F}^3}{3\pi^2} \tag{116}$$

$$k_{\rm F} = (3\pi^2 n)^{1/3} \,. \tag{117}$$

Certain authors sometimes adopt a parameter r_s to express n.

$$\frac{4}{3}\pi r_s^3 = \text{volume of a sphere of radius } r_s \,. \tag{118}$$

r_s is the radius of a sphere as large as the volume $1/n$ available to each electron:

$$\frac{4}{3}\pi r_s^3 = \frac{1}{n} \,. \tag{119}$$

Invert this relation and obtain:

$$r_s = \left(\frac{3}{4\pi n}\right)^{1/3} \,. \tag{120}$$

Note also that

$$k_{\rm F} = \left(\frac{3\pi^2}{n^{-1}}\right)^{1/3} = \left(\frac{3\pi^2}{\frac{4}{3}\pi r_s^3}\right)^{1/3} = \left(\frac{9\pi}{4}\right)^{1/3} \frac{1}{r_s} \simeq \frac{1.92}{r_s} \,. \tag{121}$$

Typical densities in ordinary metals

$$0.9 \times 10^{28} \text{ m}^{-3} \leq n \leq 2.5 \times 10^{29} \text{ m}^{-3} \tag{122}$$

correspond to

$$3 \text{ Å} \geq r_s \geq 1 \text{ Å} \,, \tag{123}$$

or equivalently

$$5.6\, a_0 \geq r_s \geq 1.9\, a_0 \,. \tag{124}$$

[Note: Wigner crystal wins for $n < 1.4 \times 10^{24}$ m^{-1}, or $r_s > 56$ Å $= 102\, a_0$, far more rarefied than standard metals!!]

In the ordinary density range

$$0.64 \text{ Å}^{-1} \leq k_F \leq 1.9 \text{ Å}^{-1} \,. \tag{125}$$

The Fermi energy

$$\epsilon_{\rm F} = \frac{\hbar^2 k_F^2}{2m_e} = \frac{\hbar^2}{2m_e} \left(3\pi^2 n\right)^{2/3} \simeq \frac{14 \text{ eV Å}^2}{r_s^2} \,. \tag{126}$$

For the relevant densities in metals one gets

$$1.6 \text{ eV} \leq \epsilon_{\rm F} \leq 14 \text{ eV} \,. \tag{127}$$

Discuss table on metals in Kittel (Chap. 6, Table 1).

Useful formula: the density of free-electron kinetic-energy states:

$$g(\epsilon) = \frac{3}{2} \, N \, \frac{\epsilon^{1/2}}{\epsilon_{\rm F}^{3/2}} \,. \tag{128}$$

In particular, the density of states at the Fermi energy can easily be obtained from Eq. (128):

$$g(\epsilon_{\rm F}) = \frac{3}{2}\,\frac{N}{\epsilon_{\rm F}}\,. \tag{129}$$

The 0-temperature total KS kinetic energy is

$$E_{\rm kin} = \frac{3}{5}\,N\,\epsilon_{\rm F} \quad \text{(from a simple } \vec{k}\text{-integration)}. \tag{130}$$

To obtain the total energy of the electrons, one should add some potential-energy. In the KS scheme the potential energy $\tilde{V}(\vec{r}) = V_{\rm ext}(\vec{r}) + V_{\rm Hartree}[\vec{r}, n_0] + V_{\rm xc}[\vec{r}, n_0]$, Eq. (86), is normally a function of position. For a homogeneous electron gas, where $V_{\rm ext}$ is a constant, $\tilde{V}$ is just a constant (i.e. position-independent) potential energy, because the ground-state density n_0 is constant too. According to Eq. (81), the total potential energy is

$$\int d^3r\, n_0 V_{\rm ext} + \frac{e^2}{2}\int d^3r \int d^3r'\,\frac{n_0 n_0}{\vec{r}-\vec{r}'} + E_{\rm xc}[n_0]\,. \tag{131}$$

Calculation of the potential-energy contributions to the total electronic energy:

$$E_{\rm Hartree}[n_0] = \frac{1}{2}\frac{1}{4\pi\epsilon_0}\int d^3\vec{r}\int d^3\vec{r}'\,\frac{[-q_e n_0(\vec{r})]\,[-q_e n_0(\vec{r}')]}{|\vec{r}-\vec{r}'|} = \frac{1}{2}e^2 n_0^2\int d^3\vec{r}\int d^3\vec{r}'\,\frac{1}{|\vec{r}-\vec{r}'|}\,. \tag{132}$$

In the thermodynamic limit of infinitely large Volume $\to \infty$ both these integrals diverge. As a result, overall this Hartree energy diverges as Volume^2! This result is embarrassing: we are happy that a total-energy contribution diverges with Volume, consistent with a finite energy density (or energy per electron). But a divergence as Volume^2 implies that the energy *density* is infinitely large!

This apparent paradox is solved by taking the positive-charge background (jellium) into account. The total adiabatic energy is an eigenvalue of

$$\hat{H}_e^{(R)} = \hat{T}_e + \hat{V}_{ee} + \hat{V}_{en}^{(R)} + \hat{V}_{nn}^{(R)} \tag{133}$$

see Eq. (11).

Consider first $\hat{V}_{nn}^{(R)}$. In real matter with discretely located nuclei at fixed positions, this contribution to $V_{\rm ad}$ would be

$$E_{nn} = \frac{1}{2}\frac{1}{4\pi\epsilon_0}\sum_{i=1}^{N_n}\sum_{j\neq i}\frac{Z_i q_e\, Z_j q_e}{|\vec{R}_i-\vec{R}_j|} = \frac{e^2}{2}\sum_{i=1}^{N_n}\sum_{j\neq i}\frac{Z_i\, Z_j}{|\vec{R}_i-\vec{R}_j|}\,. \tag{134}$$

In the jellium model we have smeared positive charge, whose electrostatic repulsion energy is:

$$E_{nn} = E_{\rm jellium} = \frac{1}{2}\frac{1}{4\pi\epsilon_0}\int d^3\vec{r}\int d^3\vec{r}'\,\frac{[q_e n_0]\,[q_e n_0]}{|\vec{r}-\vec{r}'|} = \frac{e^2}{2}\int d^3\vec{r}\int d^3\vec{r}'\,\frac{n_0^2}{|\vec{r}-\vec{r}'|}\,. \tag{135}$$

This is (of course!) exactly the same as the diverging Hartree repulsion between the uniformely distributed electrons (132).

The other missing Coulomb term is the attraction between the electrons and the jellium background:

$$E_{\rm ext} = \int d^3\vec{r}\, n_0\, V_{\rm ext} = \frac{1}{4\pi\epsilon_0}\int d^3\vec{r}\int d^3\vec{r}'\,\frac{[-q_e n_0]\,[q_e n_0]}{|\vec{r}-\vec{r}'|} = -e^2\int d^3\vec{r}\int d^3\vec{r}'\,\frac{n_0^2}{|\vec{r}-\vec{r}'|}\,. \tag{136}$$

[Notice that Eq. (136) has no 1/2 correction for double counting.] This electron-jellium term is negative (attractive), and it diverges as Volume^2 too. Clearly,

$$E_{\rm ext} + E_{\rm Hartree}[n_0] + E_{\rm jellium} = \left(-1+\frac{1}{2}+\frac{1}{2}\right)e^2\int d^3\vec{r}\int d^3\vec{r}'\,\frac{n_0^2}{|\vec{r}-\vec{r}'|} = 0\,. \tag{137}$$

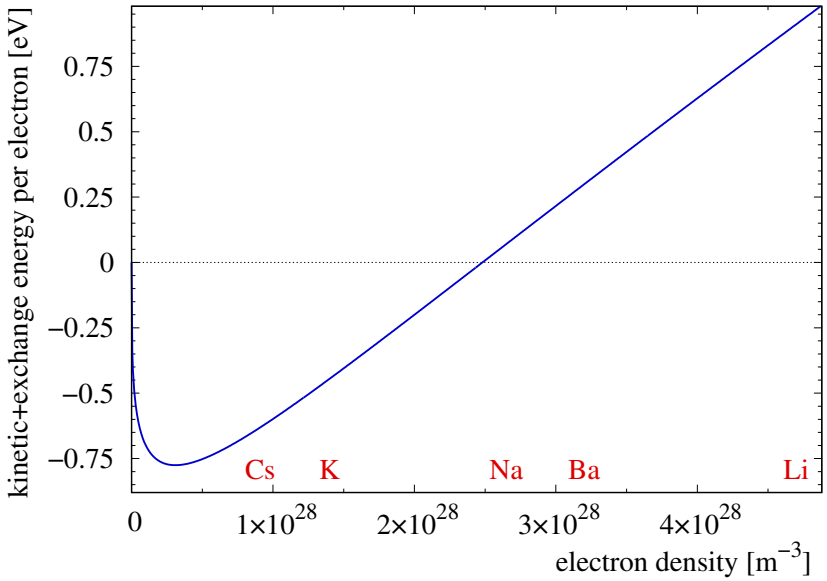

FIGURE 3.2. The sum of the kinetic plus Coulomb exchange energy contributions to the total adiabatic energy of the homogeneous electron gas, as a function of the electron density. As the classic electrostatic terms cancel exactly, this energy only neglects correlation contributions, see Sect. 2.4.3.1.

Thus we have perfect cancellation of the attractive electron-jellium term with the two repulsive electron-electron (Hartree) energy and jellium-jellium energy terms.

This takes classic electrostatics into account.

There remains the exchange & correlation energy, and this term has a correct extensive behavior, it grows as Volume (or equivalenty as N), not as Volume^2.

See Ashcroft [**2**] Chap 2 (independent electrons) and 17 (electron-electron interaction treated within a self-consistent field scheme, Hartree-Fock).

In particular, in the uniform gas, for the Slater determinant of plane waves it is possible to write an exact expression of the Fock exchange energy as

$$E_x = -\frac{3}{4\pi}e^2 k_{\rm F} N = -\frac{3}{4}\left(\frac{9}{4\pi^2}\right)^{1/3}\frac{e^2}{r_s}N = -\frac{3}{4}\left(\frac{3}{\pi}\right)^{1/3} e^2\, n^{1/3}\, N = -\frac{3}{4}\left(\frac{3}{\pi}\right)^{1/3} e^2\, n^{4/3} \times \text{Volume}\,. \tag{138}$$

Note the negative sign, and the dependence $\propto n^{1/3} \propto r_s^{-1}$ of the exchange energy per particle.

For the correlation energy we lack a similar analytic expression (just asymptotic formulas and interpolations of Monte Carlo data, see Sec. 2.4.3.1).

Leaving the correlation energy out for simplicity, the total adiabatic energy of the homogeneous electron gas also contains two terms, the kinetic energy and the exchange one:

$$E_{\rm tot} = N\left(\frac{3}{5}\epsilon_{\rm F} + \epsilon_{\rm x}\right). \tag{139}$$

We can express this energy per electron:

$$\frac{E_{\rm tot}}{N} = \frac{3}{5}\epsilon_{\rm F} + \epsilon_x = \frac{3}{5}\frac{\hbar^2}{2m_e}k_{\rm F}^2 - \frac{3}{4\pi}e^2 k_{\rm F} = \frac{3}{5}\frac{\hbar^2}{2m_e}\left(3\pi^2 n\right)^{2/3} - \frac{3}{4}\left(\frac{3}{\pi}\right)^{1/3} e^2\, n^{1/3}. \tag{140}$$

The positive kinetic term grows as $n^{2/3} \propto r_s^{-2}$, the negative exchange term grows as $n^{1/3} \propto r_s^{-1}$. At small density, the exchange term dominates.

The competition between the 2 terms gives a negative balance for $n < 2.48 \times 10^{28}$ m^{-3} (i.e. $r_s > 2.127$ Å), and positive energy above, see Fig. 3.2. The minimum of $E_{\rm tot}/N = -0.0284966\, E_{\rm Ha} = -0.775$ eV, occurs for $n = 3.1 \times 10^{27}$ m^{-3}, i.e. $r_s = 4.254$ Å. An overall negative energy, indicates that a jellium-homogeneous electron gas system (if it existed) would remain in mechanical equilibrium, thanks to the exchange energy. A positive total energy signals mechanical instability: the jellium+homogeneous electron gas would spontaneously decompose under the explosively large pressure associated to the kinetic energy of the electrons, if no other forces were there to keep it together at that density.

Be well aware of the difference between the total energy of Eq. (139), which is a macroscopic thermodynamic quantity, and the single-electron "quasiparticle band" energies:

$$\epsilon(\vec{k}) = \frac{\hbar^2 k^2}{2m_e} + \tilde{V}\,, \tag{141}$$

which are "intensive" quantities, directly comparable to the chemical potential μ. [In atoms, we similarly contrast the total energy with the individual shell levels.]

3.1.1. AC conductivity of the HEG. Alias: Kittel [**1**] Chap. 6, Problem 6.

Starting point, the electric current density:

$$\vec{j} = -q_e n \vec{v}\,. \tag{142}$$

Invert:

$$\vec{v} = \frac{1}{-q_e n}\vec{j}\,. \tag{143}$$

Equation of motion for the drift velocity $\vec{v}$:

$$m_e \left(\frac{d}{dt} + \frac{1}{\tau}\right)\vec{v} = -q_e \vec{E}\,. \tag{144}$$

Substitute Eq. (143)

$$m_e \left(\frac{d}{dt} + \frac{1}{\tau}\right)\frac{1}{-q_e n}\vec{j} = -q_e \vec{E}\,. \tag{145}$$

Simplify:

$$\left(\frac{d}{dt} + \frac{1}{\tau}\right)\vec{j} = \frac{q_e^2 n}{m_e}\vec{E}\,. \tag{146}$$

Assume a sinusoidally oscillating field

$$\vec{E} = \vec{E}_0 e^{-i\omega t}\,. \tag{147}$$

and make a corresponding ansatz for the current in the steady regime:

$$\vec{j} = \vec{j}_0 e^{-i\omega t}\,. \tag{148}$$

Substitute in Eq. (146):

$$\left(\frac{d}{dt} + \frac{1}{\tau}\right)\vec{j}_0 e^{-i\omega t} = \frac{q_e^2 n}{m_e}\vec{E}_0 e^{-i\omega t}\,. \tag{149}$$

Take the derivative and simplify the trivial factor $e^{-i\omega t}$:

$$\left(-i\omega + \tau^{-1}\right)\vec{j}_0 = \frac{q_e^2 n}{m_e}\vec{E}_0\,. \tag{150}$$

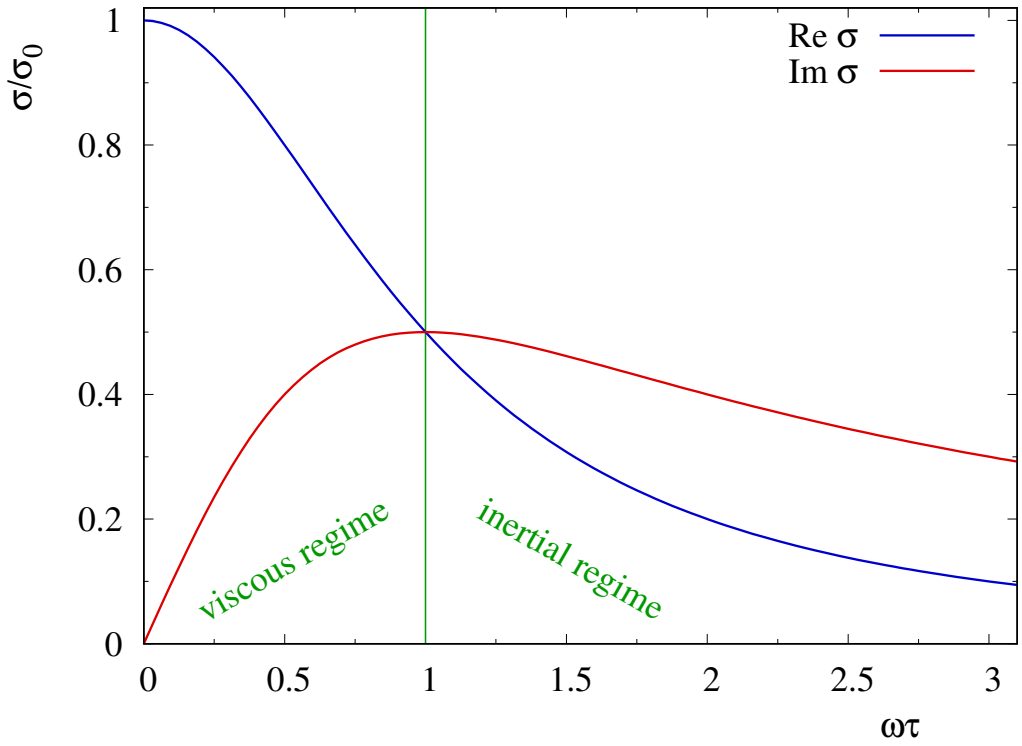

FIGURE 3.3. The frequency-dependent real and imaginary parts of the electric AC conductivity of free electrons.

Rearrange:

$$\vec{j}_0 = \frac{q_e^2 n}{m_e\left(\tau^{-1} - i\omega\right)}\vec{E}_0 = \frac{q_e^2 n}{m_e\tau^{-1}\left(1 - i\omega\tau\right)}\vec{E}_0 = \sigma_0\,\frac{1}{1 - i\omega\tau}\,\vec{E}_0\,, \tag{151}$$

where $\sigma_0 = q_e^2 n\tau/m_e$ is the usual static conductivity. Equation (151) defines a frequency-dependent complex conductivity σ. It may be convenient to separate the real and imaginary part of σ with the following trick:

$$\sigma = \sigma_0\,\frac{1}{1 - i\omega\tau} = \sigma_0\,\frac{1 + i\omega\tau}{(1 - i\omega\tau)(1 + i\omega\tau)} = \sigma_0\,\frac{1 + i\omega\tau}{1 + (\omega\tau)^2} = \frac{\sigma_0}{1 + (\omega\tau)^2} + i\,\frac{\sigma_0\,\omega\tau}{1 + (\omega\tau)^2}\,. \tag{152}$$

Figure. 3.3 reports these quantities.

Note that a complex σ indicates a dephasing of current density relative to the electric field (i.e., of the current relative to the applied oscillating voltage):

- real $\sigma \to \vec{j}_0$ and $\vec{E}_0$ have the same phase $\to \vec{j}$ and $\vec{E}$ oscillate in phase;
- $\mathrm{Re}\,\sigma \gg \mathrm{Im}\,\sigma \to \vec{j}$ is only slightly phase-delayed relative to $\vec{E}$;
- $\mathrm{Re}\,\sigma = \mathrm{Im}\,\sigma \to \vec{j}$ is phase-delayed by 45° relative to $\vec{E}$;
- $\mathrm{Re}\,\sigma \ll \mathrm{Im}\,\sigma \to \vec{j}$ is phase-delayed by 90° relative to $\vec{E}$.

3.2. Electrons in periodic crystals

3.2.1. Preliminary observations on symmetry. Recall the Kohn-Sham equation (85) (the same reasoning could be carried out within HF as well):

$$\Big(-\frac{\hbar^2}{2m}\Delta + \underbrace{V_{\mathrm{ext}}(\vec{r}) + V_{\mathrm{Hartree}}[\vec{r},n] + V_{\mathrm{xc}}[\vec{r},n]}_{\tilde{V}(\vec{r})}\Big)\phi_k(\vec{r}) = \epsilon_k\,\phi_k(\vec{r})\,. \tag{153}$$

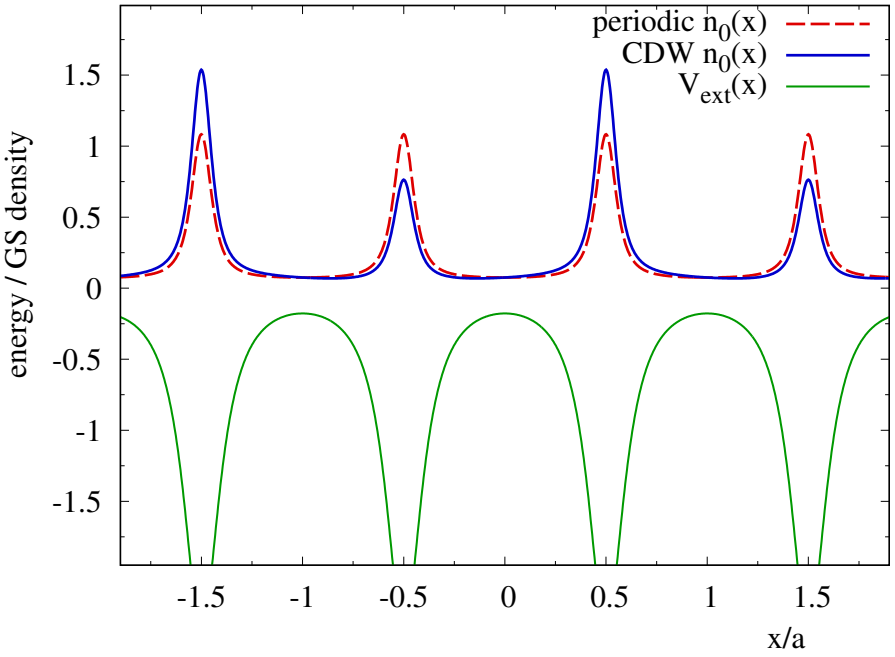

FIGURE 3.4. Two possible ground-state densities resulting from a periodic external potential: an equally-periodic density (dashed), which shares the same symmetry as the potential, and a CDW density (solid), exhibiting a doubled period. This CDW is an example of spontaneous symmetry breaking.

Here the effective potential $\tilde{V}(\vec{r}) = \tilde{V}_{\rm ext}[n_0](\vec{r})$ acts on the single-electron wave functions in the KS scheme. In a crystal, $V_{\rm ext}(\vec{r})$ is a periodic function.

If $n_0(\vec{r})$ is also periodic with the same periodicity as $V_{\rm ext}(\vec{r})$, then of course also $\tilde{V}(\vec{r})$ is.

Note the *if*. The charge density is *not* guaranteed to have the same (periodic) symmetry as the extern potential. In certain crystals, *spontaneous symmetry breaking* can occur. The density can have a lower symmetry than the extern potential. This kind of spontaneous symmetry breaking is analogous to the Wigner crystal discussed previously in the context of the electrons+jellium model.

The simplest example of charge density with lower symmetry than the external potential is a *charge-density wave* (CDW) with period doubling, as sketched in Fig. 3.4. The longest-wavelength component in the Fourier expansion of $n_0(\vec{r})$, $\vec{q}_{\rm CDW}$ is one half of some primitive reciprocal vector $\vec{b}_1$.

Several other more complicated solutions may arise in real-life 3D crystals, including nonperiodic ones, where the CDW wave vector $\vec{q}_{\rm CDW}$ is incommensurate to the $\vec{G}$ vectors of the reciprocal lattice.

A nonzero response of the lattice phonons to the charge perturbation at $\vec{q}_{\rm CDW}$ will lead to a crystal distortion, which will eventually lower the symmetry of $V_{\rm ext}(\vec{r})$ too! In the example of period doubling the resulting distortion is called Peierls dimerization.

Is the lower symmetryof $n_0(\vec{r})$ causing the ionic distortion and the ensuing structural symmmetry lowering, or vice versa? A chicken vs. egg causality dilemma...

3.2.2. The KS equation in a periodic effective potential. Assume that the total self-consistent effective potential $\tilde{V}(\vec{r})$ is indeed periodic. Then:

$$\tilde{V}(\vec{r}) = \sum_{\vec{G}} U_{\vec{G}}\, e^{i\vec{G}\cdot\vec{r}}\,, \tag{154}$$

where the sum extends over all $\vec{G}$ vectors in the reciprocal lattice. Observe that since $\tilde{V}(\vec{r}) = \tilde{V}_{\rm eff}[n_0](\vec{r})$ is real, we can be sure that $U_{-\vec{G}} = U^*_{\vec{G}}$.

The KS equation (85) can be written in the form

$$\left(-\frac{\hbar^2}{2m}\Delta + \tilde{V}(\vec{r}) - \epsilon\right)\phi(\vec{r}) = 0\,. \tag{155}$$

A smart approach to Eq. (155) comes with a Fourier expansion of its solution:

$$\phi(\vec{r}) = \sum_{\vec{k}'} C(\vec{k}')\, e^{i\vec{k}'\cdot\vec{r}}\,. \tag{156}$$

We plan to substitute both Fourier expansions in the equation (155). The kinetic term yields:

$$-\frac{\hbar^2}{2m}\Delta\phi(\vec{r}) = -\frac{\hbar^2}{2m}\Delta\sum_{\vec{k}'} C(\vec{k}')\, e^{i\vec{k}'\cdot\vec{r}} = -\frac{\hbar^2}{2m}\sum_{\vec{k}'} C(\vec{k}')\,\Delta e^{i\vec{k}'\cdot\vec{r}} = \frac{\hbar^2}{2m}\sum_{\vec{k}'} k'^2 C(\vec{k}')\, e^{i\vec{k}'\cdot\vec{r}}\,.$$

The potential term becomes

$$\tilde{V}(\vec{r})\phi(\vec{r}) = \sum_{\vec{G}} U_{\vec{G}}\, e^{i\vec{G}\cdot\vec{r}} \sum_{\vec{k}'} C(\vec{k}')\, e^{i\vec{k}'\cdot\vec{r}} = \sum_{\vec{G}}\sum_{\vec{k}'} C(\vec{k}')\, U_{\vec{G}}\, e^{i(\vec{G}+\vec{k}')\cdot\vec{r}}\,.$$

We substitute these results in Eq. (155), multiply both sides by $\exp(-i\vec{k}\cdot\vec{r})$, and integrate in $d^3\vec{r}$ over all space:

$$\int d^3\vec{r} e^{-i\vec{k}\cdot\vec{r}}\left(\frac{\hbar^2}{2m}\sum_{\vec{k}'} k'^2 C(\vec{k}') e^{i\vec{k}'\cdot\vec{r}} + \sum_{\vec{G}}\sum_{\vec{k}'} C(\vec{k}')\, U_{\vec{G}}\, e^{i(\vec{G}+\vec{k}')\cdot\vec{r}} - \epsilon\sum_{\vec{k}'} C(\vec{k}') e^{i\vec{k}'\cdot\vec{r}}\right) = 0$$

$$\frac{\hbar^2}{2m}\sum_{\vec{k}'} k'^2 C(\vec{k}')\int e^{i(\vec{k}'-\vec{k})\cdot\vec{r}}\, d^3\vec{r} +$$

$$+\sum_{\vec{G}}\sum_{\vec{k}'} C(\vec{k}')\, U_{\vec{G}}\int e^{i(\vec{G}+\vec{k}'-\vec{k})\cdot\vec{r}} d^3\vec{r} +$$

$$-\epsilon\sum_{\vec{k}'} C(\vec{k}')\int e^{i(\vec{k}'-\vec{k})\cdot\vec{r}} d^3\vec{r} = 0\,.$$

In the large-sample limit, the spatial integration produces Kronecker deltas over the momenta:

$$\int_{\text{Volume}} e^{i(\vec{k}'-\vec{k})\cdot\vec{r}}\, d^3\vec{r} = \text{Volume}\,\delta_{\vec{k}',\vec{k}} \tag{157}$$

Therefore, simplifying a common Volume factor, the $\vec{k}'$ summations disappear leaving simply:

$$\overbrace{\frac{\hbar^2}{2m}k^2 C(\vec{k})}^{\vec{k}'=\vec{k}} + \overbrace{\sum_{\vec{G}} C(\vec{k}-\vec{G})\, U_{\vec{G}}}^{\vec{k}'=\vec{k}-\vec{G}} - \overbrace{\epsilon C(\vec{k})}^{\vec{k}'=\vec{k}} = 0\,. \tag{158}$$

Precisely this disappearance of the $\vec{k}'$ summations is the consequence of the lattice periodicity of $\tilde{V}(\vec{r})$, and its resulting discrete Fourier representation. Defining

$$E^{\text{kin}}_{\vec{k}} = \frac{\hbar^2 k^2}{2m}\,, \tag{159}$$

Eq. (158) is conveniently rewritten as

$$\left(E^{\text{kin}}_{\vec{k}} - \epsilon\right) C(\vec{k}) + \sum_{\vec{G}} C(\vec{k}-\vec{G})\, U_{\vec{G}} = 0\,. \tag{160}$$

For this $\vec{k}$-space representation of the Schrödinger - KS equation, Kittel [**1**] has a special name: *central equation*. It connects a given $\vec{k}$ with all other $\vec{k}' = \vec{k} - \vec{G}$, see Fig. 7 of Chap. 7 of Kittel.

Importantly, no mixing with any other $\vec{k}$ point in the reciprocal space is provided. This is a crucial consequence of the periodicity of $\tilde{V}(\vec{r})$.

One can therefore solve Eq. (160) for a given $\vec{k}$ point in the 1BZ (combined with its $\vec{G}$-vector translations $\vec{k} - \vec{G}$), and obtain solutions:

$$\phi_{\vec{k}}(\vec{r}) = \sum_{\vec{G}} C(\vec{k}+\vec{G})\, e^{i(\vec{k}+\vec{G})\cdot\vec{r}} = e^{i\vec{k}\cdot\vec{r}} \underbrace{\sum_{\vec{G}} C(\vec{k}+\vec{G})\, e^{i\vec{G}\cdot\vec{r}}}_{u_{\vec{k}}(\vec{r}),\ \text{periodic!}} . \tag{161}$$

The function $u_{\vec{k}}(\vec{r})$ is of course periodic with the same lattice periodicity as $\tilde{V}(\vec{r})$, because all plane waves based on $\vec{G}$ vectors are periodic by definition of the reciprocal lattice. Equation (161) expresses and proves Bloch's theorem. Single-electron eigenfunctions of the Schrödinger - KS equation can always be made in the form (161). This is a consequence of the discrete translation symmetry of the effective 1-electron Hamiltonian.

Note that the contribution

$$|\phi_{\vec{k}}(\vec{r})|^2 = |e^{i\vec{k}\cdot\vec{r}}|^2\, |u_{\vec{k}}(\vec{r})|^2 \tag{162}$$

of any single-electron Bloch eigenfunction to the total electron density is necessarily periodic as well. This proves that *periodic-density solutions can certainly provide self-consistent solutions*. Also, from the practical solution side, starting from a non-GS but periodic density $n(\vec{r})$ one is certain to generate a periodic $\tilde{V}(\vec{r})$, which in turn produces new Bloch functions, a new periodic density and so on... always periodically at all steps toward the self-consistent $n_0(\vec{r})$.

Note that this observation does not rule out CDW solutions. Lower-periodicity or non-periodic solutions may be self-consistent, too. They can occasionally have lower total adiabatic energy than the periodic solution, and constitute therefore the true ground state, as e.g. in $NbSe_3$ and in 1T (trigonal) TaS_2. When simulating a solid, one should always be aware of this possibility, and verify whether it occurs.

3.2.3. Simulations of electronic KS equation in a crystal. To set up a computer simulation, one needs the following "ingredients":

(1) a simulation cell, e.g. a primitive cell in the (real-space) Bravais lattice;
(2) the atomic positions inside the cell (= the crystallographic basis), that fix $V_{\text{ext}}(\vec{r})$;
(3) a (truncated = incomplete) quantum-mechanical basis on which KS orbitals are expanded (e.g. plane waves, or atomic orbitals, or Gaussians, or...);
(4) a sampling grid in a reciprocal-lattice cell (e.g. in the 1BZ);
(5) a startup density $n(\vec{r})$ (not especially important, e.g. a uniform density is OK).

The core of the calculation is the solution of a matrix eigenvalue equation – e.g. Eq. (160) in the plane-waves quantum basis – for the expansion coefficients of the KS orbitals.

This matrix diagonalization is carried out for each $\vec{k}$ in the grid.

The computer code stores each wave function as a vector of coefficients of expansion on the basis (e.g. the $C(\vec{k}+\vec{G})$'s in the example of plane waves). This storage must be done for each $\vec{k}$ in the grid, and for each Bloch eigenstate resulting from the matrix diagonalization.

From the resulting wave functions and *the known number of electrons*, a new electron density can be computed, plugged in the Hartree and exchange&correlation functionals, a new ($\vec{k}$-dependent) matrix is generated, and the diagonalizations are redone.

This procedure is iterated again and again, with the density $n(\vec{r}) \to n_0(\vec{r})$ eventually.

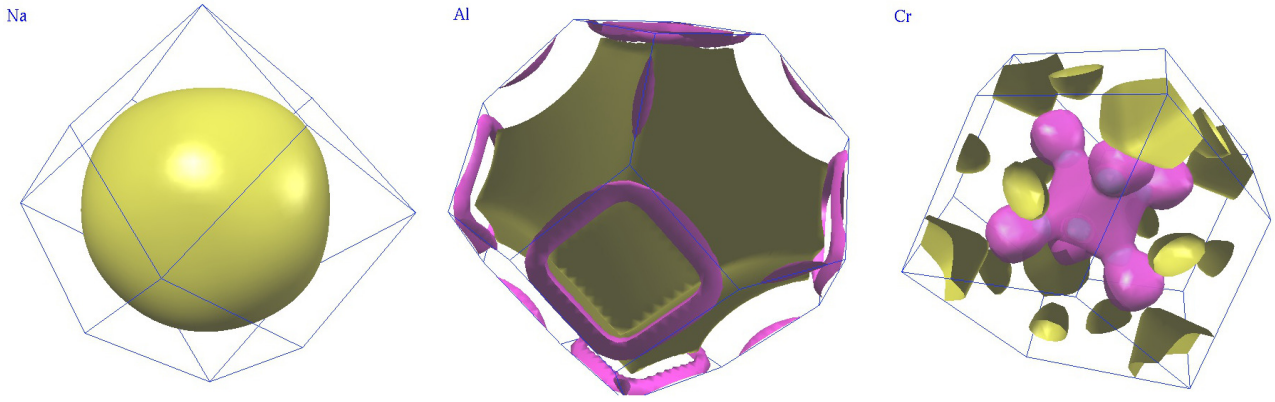

FIGURE 3.5. The Fermi surfaces of Na (bcc), Al (fcc) and Cr (bcc).

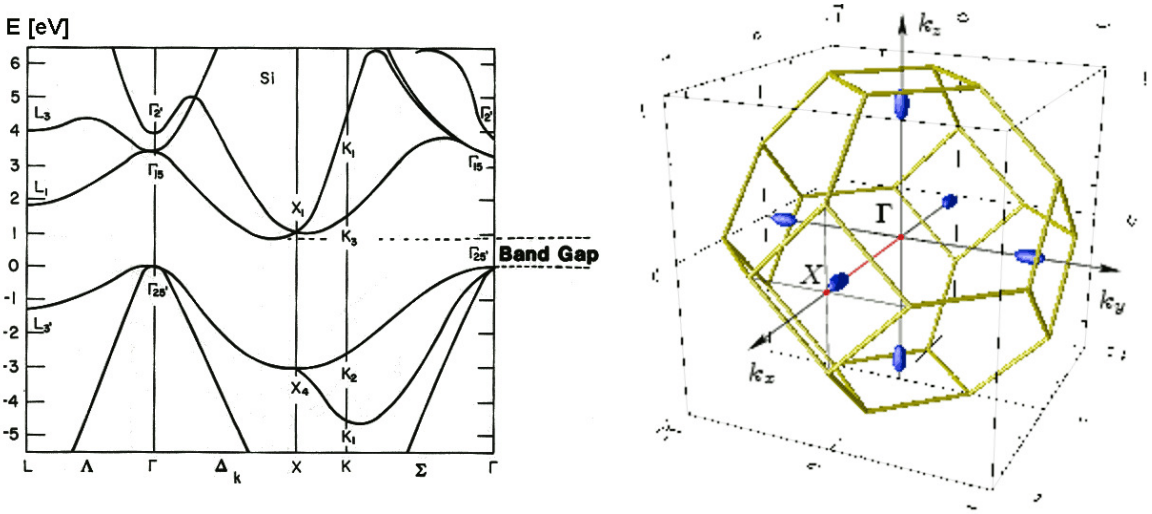

FIGURE 3.6. The silicon band structure. The energy 0 is made coincide with the top of the valence band. Note that the conduction-band minima sit at some intermediate position between Γ and X. Right: 1BZ for the fcc Bravais lattice, with the energy contour levels slightly above the conduction-band minima marked as blue surfaces.

The KS total energy $\rightarrow$ the adiabatic potential is evaluated (for this structure).

3.2.4. Fermi surfaces.

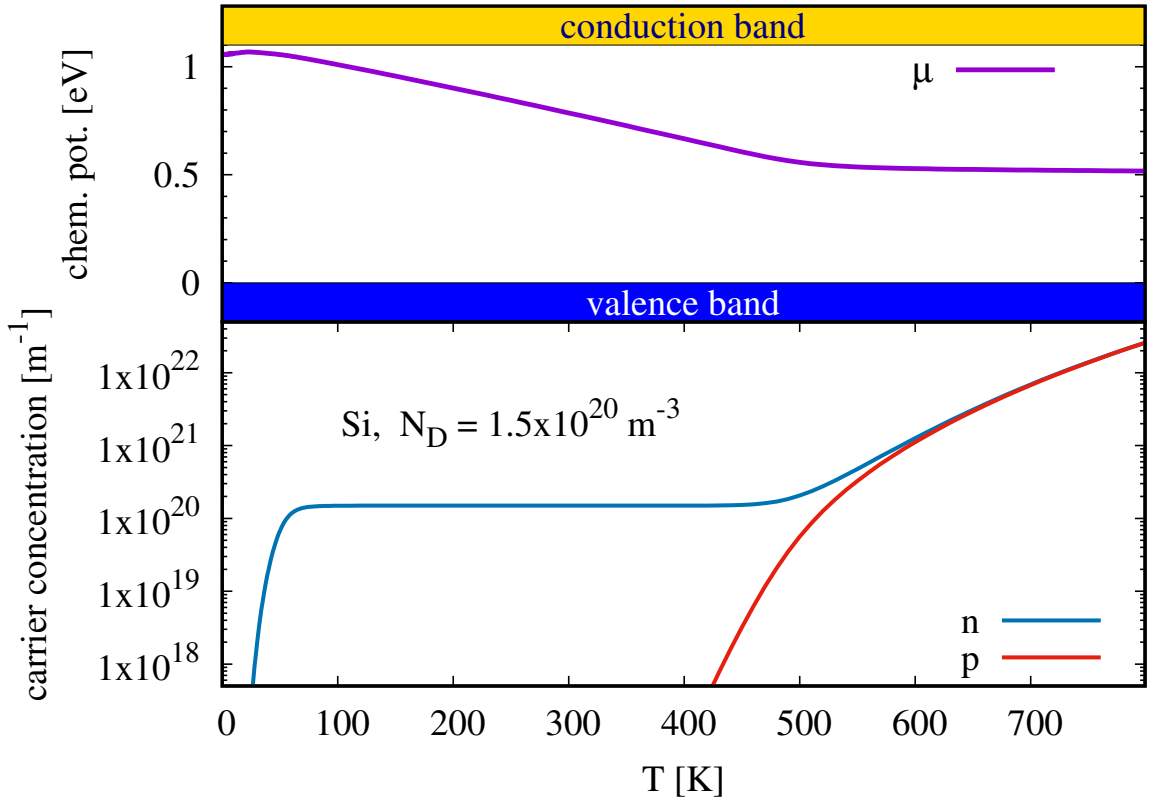

FIGURE 3.7. The temperature dependence of the chemical potential and densities of charge carriers for doped silicon in the 2-band model [**4**]. The data for this figure are obtained by means of the script `http://materia.fisica.unimi.it/manini/scripts/semiconductor_carrier_concentration.py`

CHAPTER 4

Electronic transport and optical response

4.1. Optical response of solids

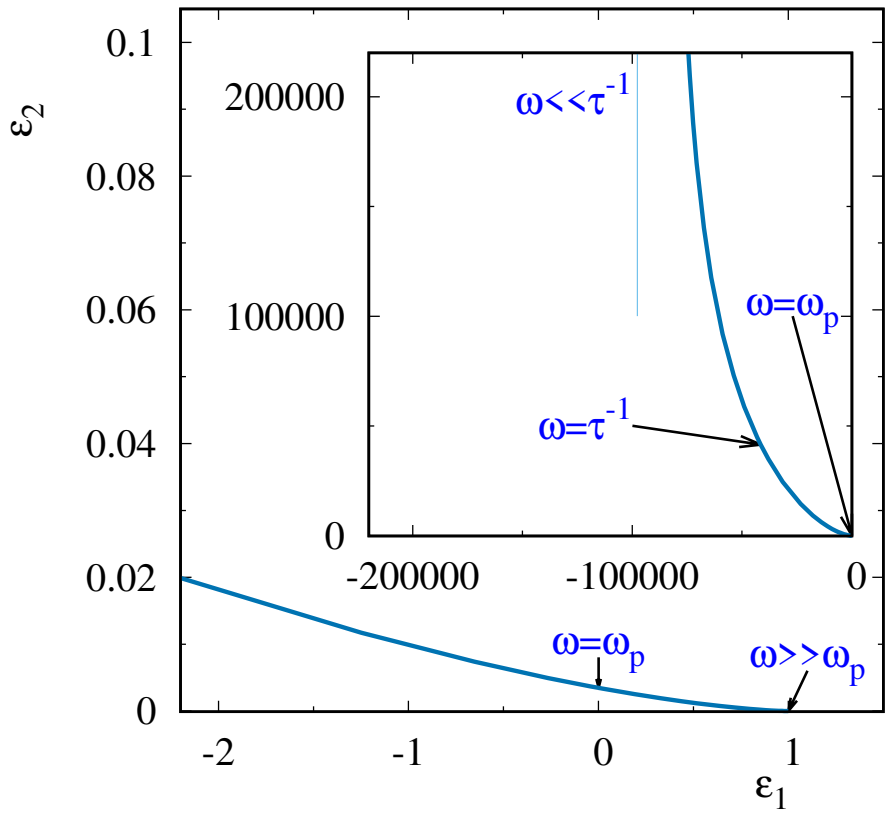

FIGURE 4.1. The complex plane, with the path that the dielectric function $\varepsilon = \varepsilon_1 + i\varepsilon_2$ of a Drude metal follows, as ω increases from 0 (left) to ∞ (right). The density $N/V \simeq 2.54 \times 10^{28}$ m^{-3} and scattering time $\tau \simeq 3.2 \times 10^{-14}$ s are those appropriate for sodium at room temperature [$\tau^{-1} \simeq 3.12 \times 10^{13}$ s^{-1}, $\omega_p \simeq 9.00 \times 10^{15}$ rad/s, corresponding to $\hbar\tau^{-1} = 0.0206$ eV, $\hbar\omega_p \simeq 5.92$ eV]. Inset: a broad-range dependence, from far infrared $\omega \ll \tau^{-1}$ to ultraviolet $\omega \gg \omega_p$; the thin line marks the vertical asymptote for $\omega \to 0$, at $\varepsilon_1 = 1 - (\omega_\mathrm{p}\tau)^2$. Main plot: a blowup of the region around ω_p.

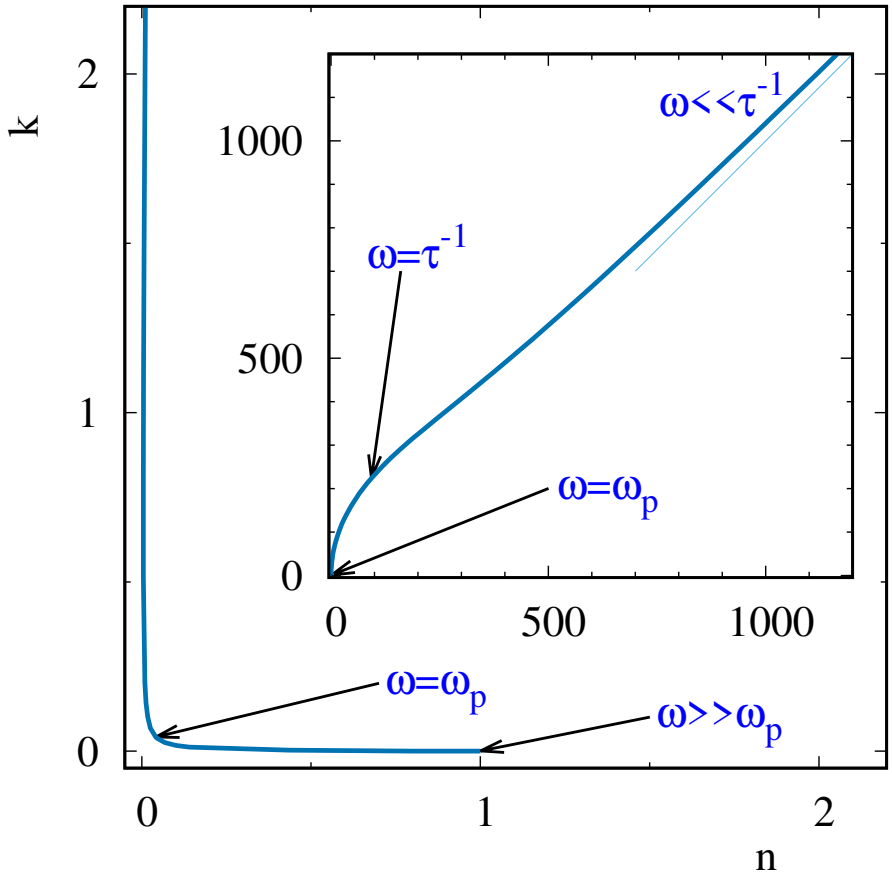

FIGURE 4.2. The path that the complex refractive index $N = n + ik = \sqrt{\varepsilon}$ of a Drude metal follows, with ω increasing from 0 (above) to ∞ (below). The density N/V and scattering time τ are the same as for Fig. 4.1, appropriate for sodium at room temperature. Inset: the overall dependence, from $\omega \ll \tau^{-1}$ to $\omega \gg \omega_p$; the thin diagonal line is the oblique asymptote for $\omega \to 0$. Main plot: a blowup of the region around $\omega_{\rm p}$.

4.2. Transport in the Boltzmann formalism

Calculations leading to Eq. (11.40) of Grosso Pastori-Parravicini [**3**]:

$$\sigma(\vec{q},\omega) = \frac{q_e^2}{4\pi^3}\int \frac{\tau v_x^2}{1 - i\tau(\omega - qv_z)}\left(-\frac{df_0}{d\epsilon}\right) d^3k \tag{163}$$

In the $T \ll T_{\rm F}$ limit

$$\sigma(\vec{q},\omega) = \frac{q_e^2}{4\pi^3}\int_{\text{Fermi surface}} \frac{\tau v_x^2}{1 - i\omega\tau + iqv_z\tau}\frac{d^2S_{\vec{k}}}{\hbar|\vec{v}|} \tag{164}$$

For a parabolic-band metal, with $\tau = \tau_F$ independent of the direction of $\vec{k}$, the Fermi surface is a sphere and spherical coordinates are recommendable for integration:

$$\begin{aligned}\sigma(\vec{q},\omega) =& \frac{q_e^2}{4\pi^3}\int_{\text{Fermi sphere}} \frac{\tau_F v_x^2}{1-i\omega\tau_F + iqv_z\tau_F}\frac{d^2S_{\vec{k}}}{\hbar|\vec{v}|} \\ =& \frac{q_e^2\tau_F}{4\pi^3\hbar}\int_{\text{Fermi sphere}} \frac{v_F^2\sin^2\theta}{1-i\omega\tau_F + iqv_F\cos\theta\tau_F}\frac{d^2S_{\vec{k}}}{v_F} \\ =& \frac{q_e^2\tau_F}{4\pi^3\hbar}v_F k_F^2\int_0^\pi d\theta\int_0^{2\pi} d\varphi \frac{\sin^3\theta\cos^2\varphi}{1-i\omega\tau_F + iqv_F\cos\theta\tau_F} \\ =& \frac{q_e^2\tau_F}{4\pi^3\hbar}v_F k_F^2\pi\int_0^\pi d\theta \frac{\sin^3\theta}{1-i\omega\tau_F + iqv_F\cos\theta\tau_F}\end{aligned} \tag{165}$$

In the last line we used $\int_0^{2\pi}\cos^2\varphi d\varphi = \pi$. We rewrite the final integration with the usual change of variable $x = \cos\theta$, implying $\sin^2\theta = 1-x^2$ and $dx = -\sin\theta d\theta$:

$$\begin{aligned}\sigma(\vec{q},\omega) =& \frac{q_e^2\tau_F}{4\pi^3\hbar}v_F k_F^2\pi\int_{-1}^1 \frac{1-x^2}{1-i\omega\tau_F + iqv_F x\tau_F}dx \\ =& \frac{q_e^2\tau_F}{4\pi^3\hbar}\frac{\hbar k_F}{m^*}k_F^2\pi\int_{-1}^1 \frac{1-x^2}{1-i\omega\tau_F + iqv_F\tau_F x}dx \\ =& \frac{q_e^2\tau_F}{4\pi^2 m^*}k_F^3\int_{-1}^1 \frac{1-x^2}{1-i\omega\tau_F + iqv_F\tau_F x}dx \\ =& \frac{q_e^2\tau_F}{4\pi^2 m^*}(3\pi^2 n)\int_{-1}^1 \frac{1-x^2}{1-i\omega\tau_F + iqv_F\tau_F x}dx \\ =& \frac{3}{4}\frac{q_e^2\tau_F n}{m^*}\int_{-1}^1 \frac{1-x^2}{1-i\omega\tau_F + iqv_F\tau_F x}dx \\ =& \frac{3}{4}\sigma_0\int_{-1}^1 \frac{1-x^2}{1-i\omega\tau_F + iqv_F\tau_F x}dx\end{aligned} \tag{166}$$

We introduce

$$s = \frac{iqv_F\tau_F}{1-i\omega\tau_F} \tag{167}$$

and rewrite

$$\sigma(\vec{q},\omega) = \frac{3}{4}\frac{\sigma_0}{1-i\omega\tau_F}\int_{-1}^1 \frac{1-x^2}{1+sx}dx \tag{168}$$

The primitive function of $\frac{1-x^2}{1+sx}$ is:

$$-\frac{x^2}{2s} + \frac{x}{s^2} + \frac{s^2-1}{s^3}\ln(1+sx) \tag{169}$$

Substitute the extremes ± 1, and obtain Eq. (11.40) of Grosso Pastori-Parravicini [**3**].

APPENDIX A

Functional Derivatives

The concept of functional derivation represent an important tool for performing minimization operations. In this appendix we provide a few useful definitions and basic results of functional calculus.

Recall the definition of the derivative of regular functions with N variables. The derivative is done with respect to one such variable, say the kth. This is the k component of the gradient of $F(u_1 \dots u_N)$, and is given by

(170)
$$\left.\frac{\partial F}{\partial u}\right|_k \equiv \frac{\partial F}{\partial u_k} = \lim_{\epsilon\to 0} \frac{F(u_1 \dots u_k + \epsilon \dots u_N) - F(u_1 \dots u_N)}{\epsilon} = \lim_{\epsilon\to 0} \frac{F(\{u_l + \epsilon\delta_{l,k}\}) - F(\{u_l\})}{\epsilon}\,,$$

where l is just a dummy component index. Functional derivatives make a generalizing step of this definition to the case of infinitely-continuously-many indexes k.

Given a set $\Omega \subseteq \mathbb{R}^n$ (a sufficiently regular domain), let us denote:

$$\mathcal{F}(\Omega) = \{u : \Omega \to \mathbb{R}\}\,, \tag{171}$$

where u are sufficiently regular functions $u(x)$. Here the continuous variable x takes the place of the discrete index k. A *functional* on Ω is a map:

$$\Phi : \mathcal{F}(\Omega) \to \mathbb{R} \quad u(x) \mapsto \Phi[u]\,. \tag{172}$$

Linear maps are simple and remarkable examples of functionals:

$$\Phi[u] = \int_\Omega dy\, g(y)\, u(y)\,, \tag{173}$$

but one easily defines nonlinear functionals too. E.g.

$$\Phi[u] = \int_\Omega dy\, g(y)\ \sin(u(y))\,, \tag{174}$$

or

$$\Phi[u] = \int_{\Omega\times\Omega} dy_1\, dy_2\, g(y_1, y_2)\, u(y_1) u(y_2)\,. \tag{175}$$

The *functional derivative* of Φ at an element u in the set of functions $\mathcal{F}(\Omega)$ which can be taken for the argument of Φ is a function $\frac{\delta\Phi}{\delta u}$ (precisely like the gradient of a scalar function of vectors $F(u)$ is a vector). Its value at point x is defined by:

$$\frac{\delta\Phi}{\delta u}[u](x) \equiv \frac{\delta\Phi}{\delta u(x)} = \lim_{\epsilon\to 0} \frac{\Phi[u(y) + \epsilon\delta(y-x)] - \Phi[u]}{\epsilon}\,, \tag{176}$$

where $y \in \Omega$ is just the dummy variable of the function argument of Φ. Here $\delta(\cdot)$ is the (n-dimensional) Dirac delta.

Let us apply this definition to a few examples. As a first example, consider an arbitrary linear functional, i.e. a functional satisfying

$$\Phi[u + v] = \Phi[u] + \Phi[v]\,, \qquad \Phi[\epsilon u] = \epsilon\Phi[u]\,. \tag{177}$$

As a consequence, applying the definition of functional derivative,

$$\frac{\delta\Phi}{\delta u(x)} = \Phi[\delta(y-x)] \,. \tag{178}$$

For the example of the linear functional in Eq. (173), we obtain

$$\frac{\delta\Phi}{\delta u(x)} = g(x) \,. \tag{179}$$

A simple special case is represented by the linear functional that selects the value of the function at one special point x_0:

$$\Phi[u] = u(x_0) \equiv \int_\Omega dy\, \delta(y-x_0)u(y) \,. \tag{180}$$

In this last formulation it comes in the form of Eq. (173), so that:

$$\frac{\delta\Phi}{\delta u(x)} = \delta(x-x_0) \,. \tag{181}$$

Another simple special case is represented by the integral:

$$\Phi[u] = \int_\Omega dy\, u(y) \,. \tag{182}$$

This is a special case of Eq. (173) with $g(x) \equiv 1$, so that:

$$\frac{\delta\Phi}{\delta u(x)} = 1 \,. \tag{183}$$

The second example is the quadratic functional of Eq. (175). For this case

$$\frac{\delta\Phi}{\delta u(x)} = \int_\Omega dy\, \left(g(x,y) + g(y,x)\right) u(y) \,. \tag{184}$$

Many remarkably important functionals take the form:

$$\Phi[u] = \int_\Omega dy\, g(y, u(y), \nabla u(y)) \,. \tag{185}$$

In this case, the functional derivative can be shown to be

$$\frac{\delta\Phi}{\delta u(x)} = \frac{\partial g}{\partial u}(x, u(x), \nabla u(x)) - \sum_{i=1}^{n} \frac{\partial}{\partial x_i}\frac{\partial g}{\partial \nabla_i u}(x, u(x), \nabla u(x)) \,. \tag{186}$$

The extension of this formalism to functionals of complex-valued functions $\{u : \Omega \to \mathbb{C}\}$ is straightforward. The most natural approach consists in considering a complex-valued $u(x)$ function as a pair of real-valued functions $u_r(x) + iu_i(x)$, and to express the functional derivative with respect to u to the functional derivatives with respect to its real and imaginary part.

To this purpose, we recall the following properties of derivation with respect to a complex variable:

$$f(z) \equiv f(z_r, z_i) = f\left(\frac{z+z^*}{2}, \frac{z-z^*}{2i}\right) \tag{187}$$

$$\frac{\partial}{\partial z} f(z_r, z_i) = f\left(\frac{z+z^*}{2}, \frac{z-z^*}{2i}\right) = \frac{1}{2}\frac{\partial f}{\partial z_r} + \frac{1}{2i}\frac{\partial f}{\partial z_i} \,. \tag{188}$$

Sumbolically, $\partial_z = \frac{1}{2}\,\partial_{z_r} + \frac{1}{2i}\,\partial_{z_i}$. Using this definition, one can immediately observe that:

$$\partial_z z = 1 \quad \partial_z z^* = 0 \,. \tag{189}$$

This formula indicates that the one can consider z^* as linearly independent of z. This is a consequence of the real and imaginary parts of a complex quantity being really independent variables.

Bringing these observations in the world of functional derivatives,

$$\frac{\delta\Phi}{\delta u(x)} \quad \text{and} \quad \frac{\delta\Phi}{\delta u^*(x)} \tag{190}$$

are fully independent functions.

Bibliography

[1] C. Kittel, *Introduction to Solid State Physics* (Wiley, New York, 2005).

[2] N. W. Ashcroft and M. D. Mermin, *Solid State Physics* (Holt-Saunders, Philadelphia, 1976).

[3] G. Grosso and G. Pastori Parravicini, *Solid State Physics* (Academic, Oxford, 2014).

[4] J. R. Hook and H. E. Hall, Solid State Physics (Wiley, Chichester, 1991).

[5] R. M. Dreizler and E. K. U. Gross, *Density Functional Theory: An Approach to the Quantum Many-Body Problem* (Springer, Berlin, 1990).

[6] M. Cinal, Phys. Rev. A **44**, 5434 (1991).

[7] L. Ravazzi, *Teoria del funzionale densità per la struttura elettronica degli atomi*, thesis (University Milan, 2019), `http://materia.fisica.unimi.it/manini/theses/ravazzi.pdf`.

[8] T. Coleman, *Thomas-Fermi model for diatomic molecules*, thesis (University Milan, 2021), `http://materia.fisica.unimi.it/manini/theses/coleman.pdf`.

[9] D. M. Ceperley and B. J. Alder, Phys. Rev. Lett. **45**, 566 (1980).

[10] J. P. Perdew and A. Zunger, Phys. Rev. B **23**, 5048 (1981).